TRANSMISSION PROPERTIES OF FISHNET STUCTURE AS A LEFT HANDED METAMATERIAL

A THESIS SUBMITTED TO
THE GRADUATE SCHOOL OF NATURAL AND APPLIED SCIENCES
OF
MIDDLE EAST TECHNICAL UNIVERSITY

BY

ŞERAFETTİN BİLGE

IN PARTIAL FULFILLMENT OF THE REQUIREMENTS
FOR
THE DEGREE OF MASTER OF SCIENCE
IN
ELECTRICAL AND ELECTRONICS ENGINEERING

FEBRUARY 2009

Approval of the thesis:

TRANSMISSION PROPERTIES OF FISHNET STUCTURE AS A LEFT HANDED METAMATERIAL

submitted by ŞERAFETTİN BİLGE in partial fulfillment of the requirements for the degree of **Master of Science in Electrical and Electronics Engineering Department, Middle East Technical University by**,

Prof. Dr. Canan Özgen
Dean, Graduate School of **Natural and Applied Sciences, Metu** _____

Prof. Dr. İsmet Erkmen
Head of Department, **Electrical and Electronics Eng., Metu** _____

Prof. Dr. Gülbin Dural
Supervisor, **Electrical and Electronics Engineering, Metu** _____

Examining Committee Members:

Prof. Dr. Gülbin Dural
Electrical and Electronics Engineering Dept., METU _____

Prof. Dr. Gönül Turhan Sayan
Electrical and Electronics Engineering Dept., METU _____

Prof. Dr. Mustafa Kuzuoğlu
Electrical and Electronics Engineering Dept., METU _____

Prof. Dr. Ekmel Özbay
Electrical and Electronics Engineering Dept., Bilkent Univ. _____

Hümeyra Çağlayan, M.Sc.
Physics Dept., Bilkent Univ. _____

Date: February 11, 2009

I hereby declare that all information in this document has been obtained and presented in accordance with academic rules and ethical conduct. I also declare that, as required by these rules and conduct, I have fully cited and referenced all material and results that are not original to this work.

Name, Last name : Şerafettin, BİLGE

Signature :

ABSTRACT

TRANSMISSION PROPERTIES OF FISHNET STUCTURE AS A LEFT HANDED METAMATERIAL

Bilge, Şerafettin

M.Sc., Department of Electrical and Electronics Engineering

Supervisor: Prof. Dr. Gülbin Dural

February 2009, 59 pages

Left handed metamaterials are one of the most populer topic attracting attentions of scientists nowadays. Metamaterials are engineered materials which can possess inordinary properties when compared with common materials existing in nature. The main structure investigated in this thesis is fishnet metamaterial which is a left handed metamaterial. Firstly some left handed metamaterials and their properties are surveyed. A retrieval procedure in order to obtain permittivity, permeability and refractive index of any periodic material was summarized. Left handedness of fishnet structure was investigated and proven numerically. Effects of change in polarization of an incoming wave to symmetric and asymmetric fishnet structure were searched. A parametric analysis of fishnet structure was done. Phase advance in a three layered fishnet structure was investigated and compared with phase advance in an ordinary material. Fishnet

wedge structure was surveyed and negative refraction and negative phase advance in this structure are shown. Finally, some types of disorderness of fishnet structure, then its effects on transmission results and retrieval results are demonstrated. In order to obtain transmission and reflection through a material, CST Microwave Studio[44] was used. A code following a numerical procedure in order to retrieve constitutive parameters of a periodic structure which was written in Matlab® was used in this thesis.

Keywords: Metamaterial, Fishnet Structure, Left handed structure, Fishnet wedge structure, Disorder

ÖZ

SOLAK BİR METAMALZEME OLAN BALIKAĞI YAPISININ GEÇİRGENLİK ÖZELLİKLERİ

Bilge, Şerafettin

Yüksek Lisans, Elektrik ve Elektronik Mühendisliği Bölümü

Tez Yöneticisi: Prof. Dr. Gülbin Dural

Şubat 2009, 59 sayfa

Solak metamalzemeler bugünlerde bilim adamlarının dikkatini çeken en popüler konulardan biridir. Metamalzemeler üretilmiş malzemeler olup doğada bulunan malzemelerle kıyaslandığında olağandışı özelliklere sahip olabilmektedirler. Bu tezde incelenen esas yapı bir solak metamalzeme olan balıkağı metamalzemesidir. Öncelikle bazı solak metamalzemeler ve özellikleri incelenmiştir. Herhangi bir periyodik malzemenin dielektrik geçirgenlik katsayısını, manyetik geçirgenlik katsayısını, kırılma indisini bulmak için bir prosedür özetlenmiştir. Balıkağı yapısının solaklığı incelenmiştir ve nümerik olarak ispatlanmıştır. Simetrik ve asimetrik balıkağı yapısına gelen dalganın polarizasyonundaki değişimin etkileri incelenmiştir. Balıkağı yapısının parametrik bir analizi yapılmıştır. Üç katmanlı bir balıkağı yapısındaki faz ilerlemesi incelenmiş ve doğal bir malzemedeki faz ilerlemesiyle karşılaştırılmıştır. Balıkağı prizma yapısı incelenmiş ve bu

yapıdaki negatif kırılma ve negatif faz ilerlemesi gösterilmiştir. Son olarak balıkağında olabilecek bazı düzensizlik çeşitleri, sonra geçirgenlik sonuçları ve elde edilen katsayılar (elektrik geçirgenlik, manyetik geçirgenlik katsayıları gibi) üzerine etkileri gösterilmiştir. Malzemenin geçirgenliği ve yansıması CST Microwave Studio[44] kullanılarak hesaplanmıştır. Bu tezde, Matlab®'da yazılmış olan ve bazı katsayıları (elektrik geçirgenlik, manyetik geçirgenlik katsayıları gibi) hesaplamak için nümerik bir prosedür izleyen bir kod kullanılmıştır.

Anahtar Sözcükler: Metamalzeme, Balıkağı Yapısı, Balıkağı Prizma Yapısı, Düzensizlik

To my family, and my beloved friend Reha Ekin Yılmaz

ACKNOWLEDGEMENTS

I would like to express my sincere gratitude to my supervisor Prof. Dr. Gülbin Dural for her guidance and help throughout the thesis work. I would also like to acknowledge valuable advice and help from Prof. Dr. Ekmel Özbay. His support, guidance, encouragements and suggestions taught me much about systematically approaching to research study. I would also like to acknowledge valuable help from Dr. Koray Aydın, and Humeyra Çağlayan. I am grateful to Nanotechnology Research Center (NANOTAM) for the facilities and working environment provided for me to perform the research study.

I would present my special thanks to my parents, Behiye and Selamet Bilge; and to my beloved friend Reha Ekin Yılmaz from Harvard University Computer Programming for their endless support and encouragement.

TABLE OF CONTENTS

LIST OF FIGURES

CHAPTER 1

INTRODUCTION

1.1 Left-handedness and its historical background

It is a well-known fact that refractive index of a medium is one of important parameters which determines how an electromagnetic wave behaves in this medium. This property (n) is determined by electrical and magnetic properties of medium called dielectric permittivity (ε) and magnetic permeability (μ), with the formula

$$n = \sqrt{\varepsilon_r \mu_r} \qquad (1.1)$$

There are four combinations for ε, μ: ε negative μ positive, ε positive μ negative, both negative and both positive. ε negative, μ positive and double positive materials are common materials existing in nature. For example, many metals have negative ε at visible spectrum[1]. But, there is no natural ε positive μ negative and both negative material. Because of this, these materials are called metamaterials. “meta” has the meaning “beyond” in Greek, that metamaterials refer to engineered materials.

A material having ε and μ that are both negative has negative refractive index. Some other names for these materials are “double negative materials”, “left-handed materials”, “backward wave materials” in literature. Left handed materials have some unique properties. One of them is existence of anti-parallelism of energy flow and wave vector in these media[2, 4]. This is called backward wave property. Some other very interesting properties of left handedness are the reversal of the Doppler shift for radiation[3], and the reversal of Cherenkov radiation[41]. Moreover, these materials promise some exciting phenomena such as subwavelength imaging[35] and cloaking[33].

Veselago who is a Russian scientist discussed the properties of electromagnetism in a double negative medium theoretically in 1968[24]. Until a time when Pendry *et al.* discussed it again in 1996, this phenomenon wasn’t in mind. Pendry *et al.* constructed these metamaterials artificially in his studies[25, 26]. Then, D. R. Smith did the first experimental realization of negative refraction in 2000[27]. The structures first engineered showed negative refractive index or negative magnetic permeability (μ) when exited with electromagnetic wave possessing normal to plane magnetic field[28]. Then Shalaev proposed a new type of structure which can show negative magnetic permeability (μ) when excited with normal to plane propagation[5]. This research area is still popular.

1.2 What does this thesis cover?

Current thesis covers five chapters. The first chapter introduction. In introduction chapter, the concept of left handedness, some interesting properties of left handed materials and history of progression for this topic was explained.

In second chapter, some left handed structures and their properties are discussed. In introduction part, some reported properties of some structures such as Split Ring Resonator (SRR), wire, SRR-Wire composite metamaterial (CMM), cutwire, cutwire-wire CMM is explained. Moreover, a retrieval procedure in order to obtain

constitutive parameters (permittivity, permeability, refractive index, impedance) of a bulk structure is summarized in introduction. In second part of second chapter, simulation and retrieval results of structures explained in introduction are comparatively discussed.

In the third chapter, fishnet structure is explained. In the introduction part, some properties of fishnet structure are explained. Variations of fishnet structure reported in the literature are shown. An equivalent circuit shown in the literature is explained. A condition for left handedness explained in literature is shown. As a second part, left handedness in fishnet structure is discussed. In this part, double negativity of fishnet structure is discussed with simulation and retrieval results. Experimental and retrieval verification of fishnet structure is shown. Polarization effects on fishnet structure are explained with a numerical calculation and simulation results. As a third part, parametric analysis of fishnet structure is done.

In the fourth chapter, negative refraction and negative phase advance of fishnet structure is discussed. In introduction part, positive and negative refraction through a triangular prism is discussed with Snell's law. In second part, phase advances through a four layered fishnet structure, and a dielectric structure are discussed with the aid of simulation results. In the third part, refraction properties and phase advance in fishnet wedge structure is analyzed with the aid of 2-D simulation results.

In the fifth chapter, disorder and in fishnet structure and its results is discussed. An introduction including motivation of this chapter is done. In second chapter, some possible disorders in fishnet structure are analyzed with the aid of experiment, simulation and retrieval results.

The sixth chapter is the conclusion chapter.

CHAPTER 2

LEFT HANDED STRUCTURES AND THEIR PROPERTIES

2.1 Introduction

2.1.1 SRR, Wire and SRR-Wire (CMM) arrays:

Left handed materials (LHM) are negative indexed materials which do not exist naturally. In order to achieve left handedness, negative permittivity and negative permeability are necessary simultaneously[2, 4, 24]. Negative permittivity was achieved with using wire structures[7, 28, 36] (see fig. 2.1a). Then, negative permeability was done with using split ring resonator (SRR) which consists two rings one inside other, splitted at opposite sides[26, 36, 28] (see fig. 2.1b). After all, negative index was achieved by combining these two structures[27, 28, 37] (see fig. 2.1c).

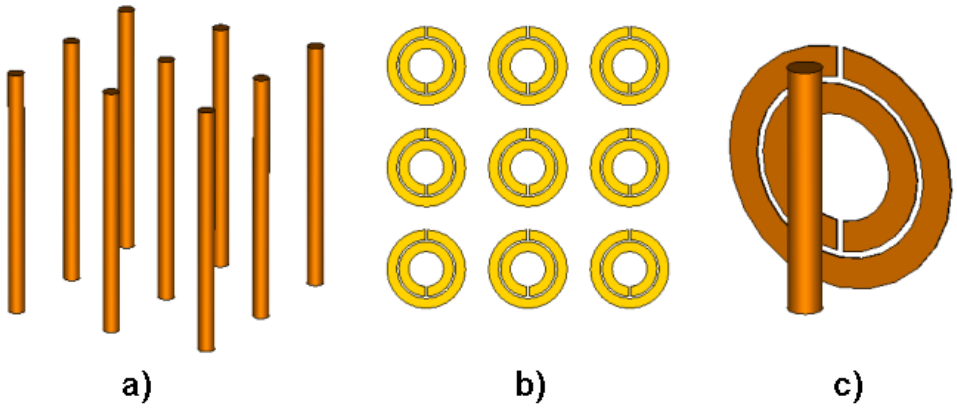

Figure 2.1 Schematics for a) wire array, b) SRR array, c) composite metamaterial (CMM).

There is a condition for an array of a structure to be accepted as an effective medium. This condition is called effective medium theory[6, 28]. According to the effective medium theory, if the wavelength of incoming wave is much larger than the largest size of a unit cell of a structure array, the medium can be treated as a homogeneous substance with an effective dielectric permittivity and effective magnetic permeability.

Exciting wire array with a wave polarized parallel to wires, gives a transmission result like a high pass filter[7]. Real part of effective permittivity of this structure is negative at the stop-band region of these transmission spectra. The frequency at the passing between stopband and passband is called plasma frequency[38]. In other words, real part of effective permittivity is negative below plasma frequency, and positive above plasma frequency. Plasma frequency[38] represents electric resonance frequency.

Exciting SRR array with a wave having a magnetic field normal to SRR plane results a transmission spectra like a notch filter[29]. The frequency at the stopband of the transmission spectra is called magnetic resonance frequency. Real part of effective magnetic permeability is negative at this stopband region of transmission spectra. An SRR array also has electric resonance frequencies[26]. In order to differentiate whether a band gap is electric resonance or magnetic resonance, one can close the splits of SRR which is called closed ring resonator (CRR) [28, 30, 40]. This method kills all magnetic resonances of SRR, in turn the band gaps which exist in transmission spectra of SRR; and don't exist in transmission spectra of CRR are magnetic resonance originated[28, 30, 40].

Combination of metamaterials is called composite metamaterial (CMM), in this case CMM is combination of SRR and wire structures[30, 37, 28]. CMM array has negative effective index in the frequency region which coincides with stopbands of only SRR array and only wire array[6, 28, 29], where the first experimental realization of negative effective index was done by D. R. Smith in 2000[27]. There is a peak at this frequency band where effective index is negative. One can understand whether this peak is left handed or not, by closing splits of SRR. If closing splits removes this peak, this peak is left handed[28, 30, 40].

2.1.2 Cutwire and CMM arrays

An SRR array can have effective negative permeability if it is excited with a wave possessing normal to plane magnetic field. An alternative structure in order to obtain

effective negative permeability was proposed by Shalaev[5]. This structure is cutwire array where one needs normal to plane propagated wave in order to obtain effective negative permeability.

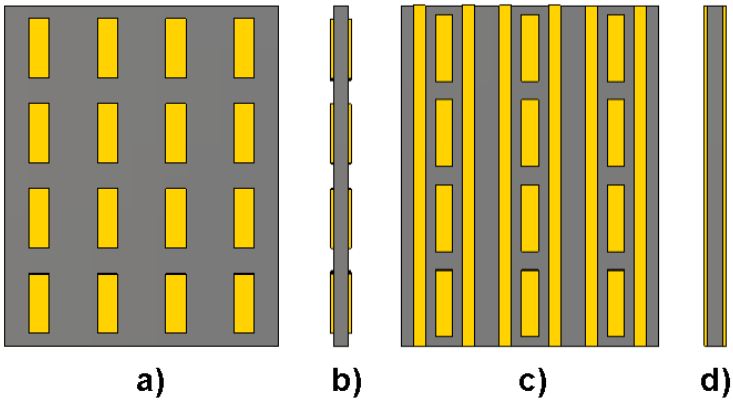

Figure 2.2 Schematics showing a) front view of cutwire array, b) side view of cutwire array, c) front view of CMM, and d) side view of CMM.

The cutwire array consisting two cutwire pairs is placed at back and front faces of a dielectric board with mirror symmetry (see fig. 2.2a and 2.2b). This structure has a magnetic resonance bandgap response if it is excited with a normal to plane propagated wave[8], in turn it has effective negative permeability in this bandgap frequency region.

In order to obtain effective negative index with using cutwire array, one should complete effective negative permittivity part. The complementary part is wire array. The resulting structure to achieve effective negative index is CMM array[9] (see fig. 2.2c and 2.2d). Transmission spectra of this structure have a peak in the effective negative index region[9].

Widening the cutwire pair and wire pair until they touch neighboring pairs results in a new structure called fishnet structure[10] (See fig. 2.3).

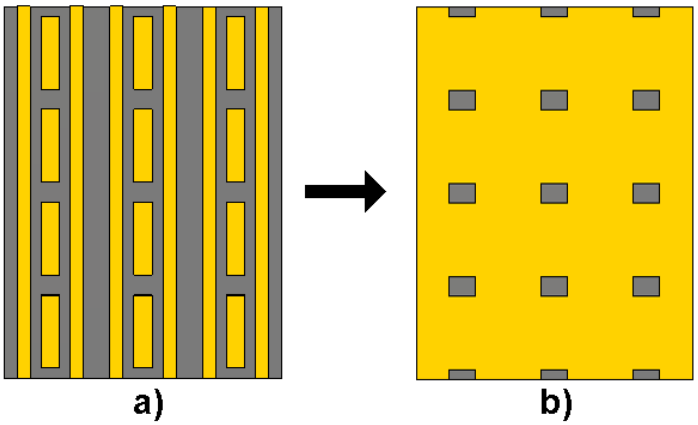

Figure 2.3 Schematics showing a) CMM array, and b) fishnet structure.

2.1.3 Retrieval Procedure

Retrieving constitutive parameters are needed in order to characterize LHMs better. S parameters of a normal to plane wave incident on a slab metamaterial are needed to achieve a retrieval procedure[11, 36, 39]. Then, refractive index n and impedance z should be calculated by using S parameters calculated before. The knowledge of refractive index n and impedance z can be used in order to calculate permittivity ε and permeability μ by using the formulas $\mu = nz$ and $\varepsilon = n/z$.

S parameters of an incident wave normal to plane of a slab can be calculated numerically. In order to obtain refractive index n and impedance z, one can use equation set 2.1.

$$z = \pm\sqrt{\frac{(1+S_{11})^2 - S_{21}^2}{(1-S_{11})^2 - S_{21}^2}} \qquad (2.1a)$$

$$n = \frac{1}{k_0 d}\{[[ln(e^{ink_0 d})]'' + 2m\pi] - i[ln(e^{ink_0 d})]'\} \qquad (2.1b)$$

$$e^{ink_0 d} = \frac{S_{21}}{1 - S_{11}\frac{z-1}{z+1}} \qquad (2.1c)$$

Where, where k_0 is free space wave number and notations $(.)'$ and $(.)''$ denotes real

and imaginary parts of any function respectively. However, equation set 2.1 is not satisfactory to finish retrieval procedure. One should find branch of impedance z and m which is branch of refractive index n in order to finish retrieval procedure. One can use equation 2.2a and 2.2b to find branch of z and m, respectively.

$$|e^{ink_0 d}| \leqslant 1 \qquad (2.2a)$$

$$|n'z''| \leqslant n''z' \qquad (2.2b)$$

After these steps, one can find permittivity ε and permeability μ by using formulas shown above.

2.2 Simulations and retrieval results of some metamaterials

2.2.1 Wire array

In order to find plasma frequency, refractive index and constitutive parameters of a medium, we can use a retrieval procedure[11]. To achieve this procedure we need to obtain both magnitude and phase values of transmission and reflection values. A simulation in order to obtain transmission and reflection results were done in CST Microwave Studio[44].

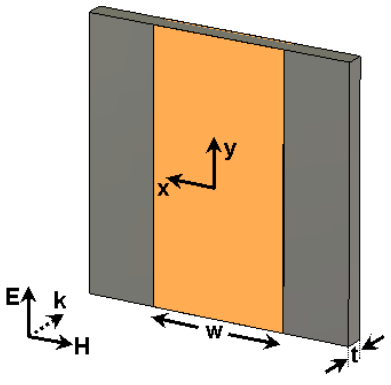

Figure 2.4 Schematic showing the one unit cell of continuous wire array.

CST Microwave Studio[44] has an algorithm that can generate 3-D spatial discrete mesh with finite integration method and perfect boundary approximation. In the

simulation, the medium filling spaces between PEC is air. Unit cell of wire medium used in simulation is shown in fig. 2.4. The unit cell includes a teflon plate coated with metal sheet lying in electric field direction at both faces. The reason for the choice of a metal sheet instead of a wire is that a continuous metal sheet lying in electric field direction behaves like a wire. The orange part in fig. 2.4 is metal sheet, and the gray part is teflon. Parameters of teflon are $\varepsilon = 2.16$, $\mu = 1$, and $\delta = 0.005$. The unit cell is periodic in x and y directions and metal sheet is continuous in y direction. Periodicities in x and y directions are both 14 mm. Thickness of metal sheet is 50 μm. The parameters shown in fig. 2.4 are w=7 mm and t=1 mm. Electric field of incident TEM wave is in y direction while propagation direction is z direction.

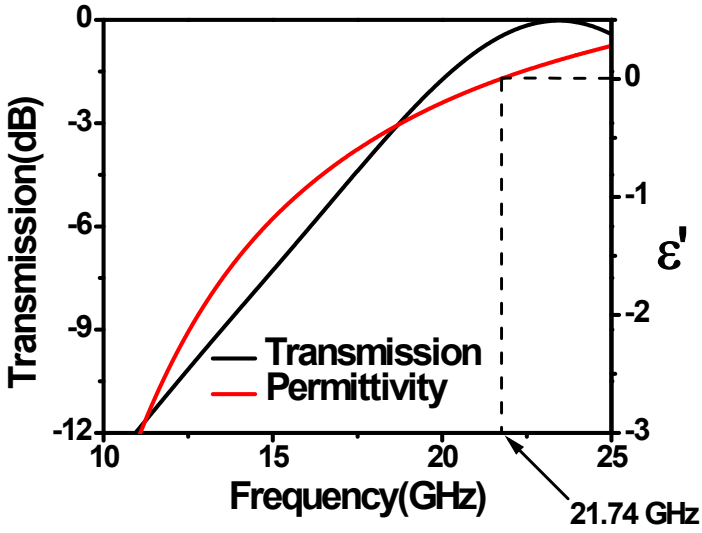

Figure 2.5 Graph showing the transmission and retrieval results for continuous wire array.

Transmission and retrieval results of continuous wire array are shown in fig. 2.5. Effective permittivity results were obtained by retrieval procedure, which is done in Matlab® using aforementioned retrieval procedure. According to inset of fig. 2.5 plasma frequency of this structure is 21.74 GHz.

As seen, up to a certain frequency the structure is opaque to electromagnetic wave. This opacity region coincides with permittivity values less than zero which can be inspected by the comparison between transmission and retrieval results shown in inset of fig. 2.5. As a result, continuous wire structure is opaque to electromagnetic wave in negative epsilon frequency region.

2.2.2 SRR array

An SRR array fixed on a lossy FR-4 board can have negative effective permeability values at a frequency band if the dimensions of structure and orientation of wave sent are chosen true.

The true dimensions for SRR in order to have negative effective permeability should satisfy effective medium theory. The true orientation of TEM wave sent in order to satisfy negative permeability, should be in the way that magnetic field is perpendicular to plane of SRR.

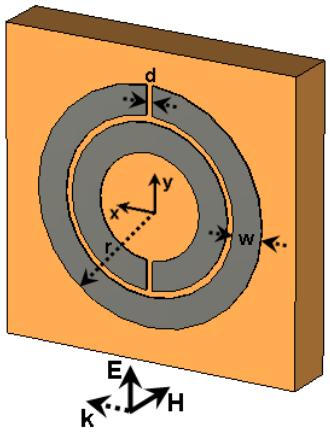

Figure 2.6 Schematic showing unit cell and dimensions of SRR structure.

One unit cell for SRR medium used in simulation is shown in fig. 2.6. In order to find the negative permeability region, one needs transmission spectra of this structure. According to simulation done, the geometrical parameters of SRR are defined in fig. 2.6. The gap between rings and the splits have the same magnitude d = 0.2 mm. Metal width is w = 0.9 mm, and the radius of the SRR is r = 3.6 mm. The

structure is one layer in the x direction. This structure is also periodic in y and z directions, and periodicities are 9.3 and 4 mm respectively. The thicknesses for metal and lossy FR-4 substrate are 50 μm and 2.6 mm respectively. Parameters of FR-4 are $\varepsilon = 4.9$, $\mu = 1$, and $\delta = 0.025$. Orientation of plane wave sent to this structure is shown in fig. 2.6. The resulting transmission graph is shown in inset of fig. 2.8, below.

The expected transmission spectrum for a magnetic resonant structure looks like a notch filter's[29] transmission spectra near magnetic resonance frequency. The black line in the inset of fig. 2.8 may belong to a magnetic resonant structure. In order to be sure whether this bandgap belongs to electric or magnetic resonance, there is a way. Closing the splits of SRR kills all magnetic[28, 30, 40] resonance bandgaps, and almost doesn't destruct any electric resonance bandgap. Thus, if one examines the difference between transmissions of SRR and CRR (closed ring resonator), then can decide type of resonance between electric and magnetic resonances.

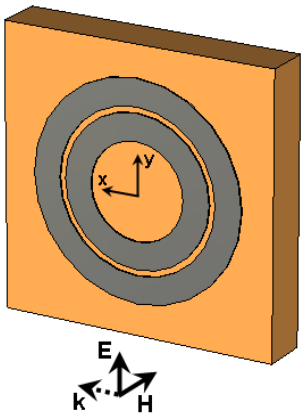

Figure 2.7 Schematic showing unit cell of CRR (Closed ring resonator) array.

The only difference between unit cells of SRR and CRR is the split (see the difference between fig. 2.6 and fig. 2.7). The resulting graph for comparison between SRR and CRR transmissions is shown in fig. 2.8.

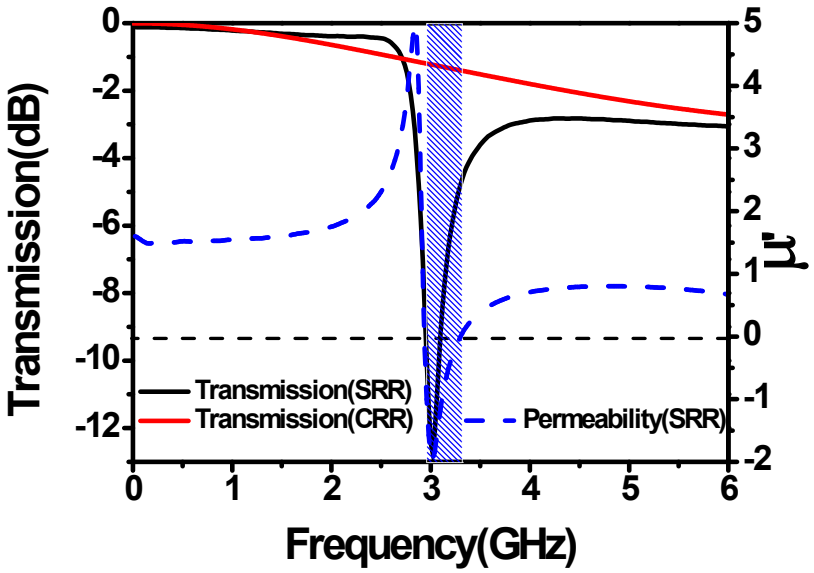

Figure 2.8 Comparison of transmission spectra of SRR and CRR arrays.

As can be seen in fig.2.8, bandgaps of SRR doesn't coincide with CRR transmission result. Thus, this bandgap is magnetic resonance region of this structure and incident wave configuration. According to fig. 2.8 magnetic resonance of the SRR shown is at 3.02 GHz. Permeability is negative only in the magnetic resonance region which is between 2.93 and 3.3 GHz as shown in fig. 2.8 with dashed blue line.

As a result of comparison between retrieval results and transmission results of SRR array, in the frequency region where permeability is negative, the structure is opaque[1] to electromagnetic waves.

2.2.3 Cutwire array

The unit cell of cutwire array comprises two metal pairs filled with dielectric in between.

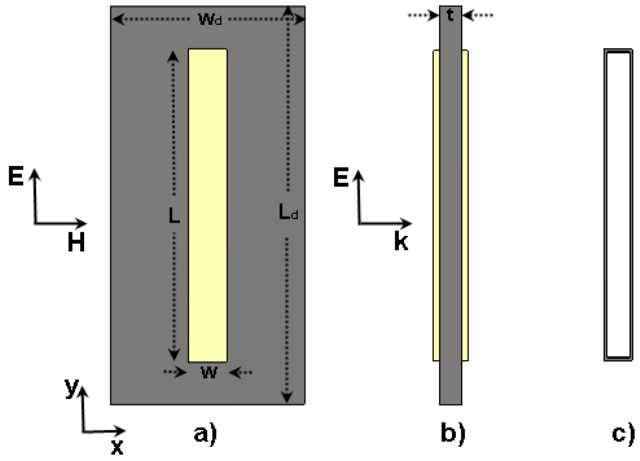

Figure 2.9 Schematics showing a) front view of cutwire pair, b) side view of cutwire pair, c) side view of closed cutwire pair.

In fig. 2.9a and 2.9b, one can see front and side views of a one unit cell of cutwire pair (cwp). Cutwire medium can have negative permeability near magnetic resonance frequency of this structure when excited with a normal to plane propagated plane wave. Similar to SRR, cutwire structure can have also electric resonances. In order to distinguish which bandgap in transmission spectrum is magnetic, one can close cutwire pairs. Cut wire pair can be closed by merging metal pair with additional metals through dielectric. After merging, the side-view of merged metal parts is seen in fig. 2.9c where dielectric part is hidden (see the difference between fig. 2.9b and fig. 2.9c by ignoring dielectric).

The dimensions of the structure used in the simulation are, L=5.5 mm, w=1 mm, L_d = w_d = 7 mm, t_m (thickness of metal) = 50 μm, t_d (thickness of dielectric) = 1 mm. Periodicities in x and y directions are 7 mm. Parameters of the dielectric are $\epsilon = 4.9$, $\mu = 1$, and $\delta = 0.025$. The structure is periodic in x and y directions. The resulting comparative transmission graph is show in fig. 2.10.

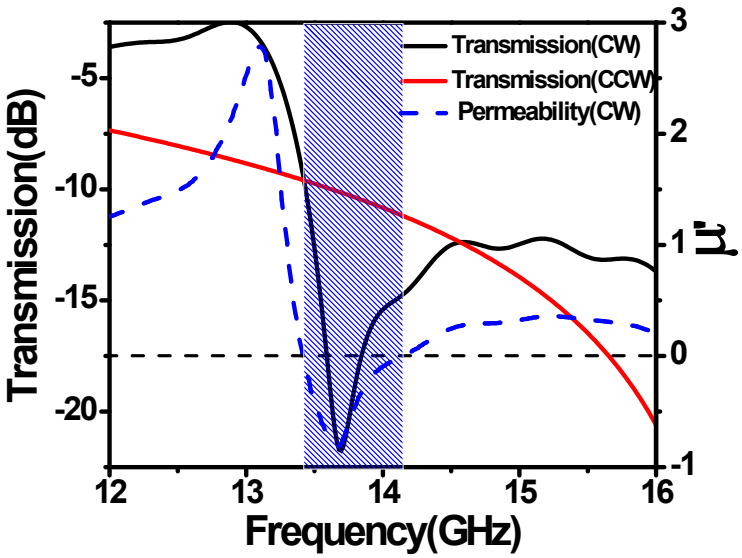

Figure 2.10 Graph showing transmission results of cutwire and closed cutwire arrays, and permeability result of cutwire structure.

The sharp transmission bandgap in fig. 2.10 (black line) is magnetic originated since no bandgap exists in transmission graph of closed cutwire pair (red line) where a bandgap exists in transmission graph of cutwire structure (black line). The resulting magnetic resonance frequency of this structure is 13.7 GHz.

This structure possesses negative permeability between 13.41 and 14.14 GHz, where minimum permeability is -0.816 at 13.66 GHz which can be seen in fig. 2.10. As a result of comparison between transmission and permeability results of cutwire array, the negative permeability frequency region is opaque to electromagnetic wave; in turn electromagnetic wave is evanescent in cutwire structure in negative permeability frequency region.

2.2.4 SRR-Wire array

The CMM array is a LHM in a frequency band when excited with a plane wave possessing normal to plane magnetic field.

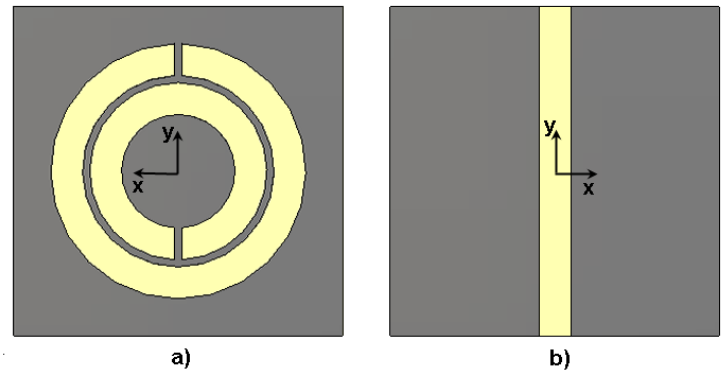

Figure 2.11 Schematics showing a) front view, and b) back-view of CMM array.

One unit cell of a SRR-Wire structure is shown in fig. 2.11. Fig. 2.11a and 2.11b show front face and back face of unit cell respectively. In the simulation, propagation is in x direction and polarization is in y direction (one can see x, y and z axes in fig. 2.11). The structure in simulation involves one unit cell in z direction. The periodicities are the same as only SRR structure mentioned before. The dimension of SRR and type of dielectric is the same as the SRR structure. The width of the wire is 0.9 mm.

Double negativity exists only at a narrow band, because negative permeability can exist only in a narrow frequency band. In contrast with a medium having only negative medium, a double negative medium is transparent to electromagnetic wave. As can be seen in fig. 2.12, at the intersection of stopbands of permittivity and permeability results (green and light blue lines) transmission is high enough (between -1.6 and -7.8 dB), in turn the structure is transparent to electromagnetic wave in double negative frequency region.

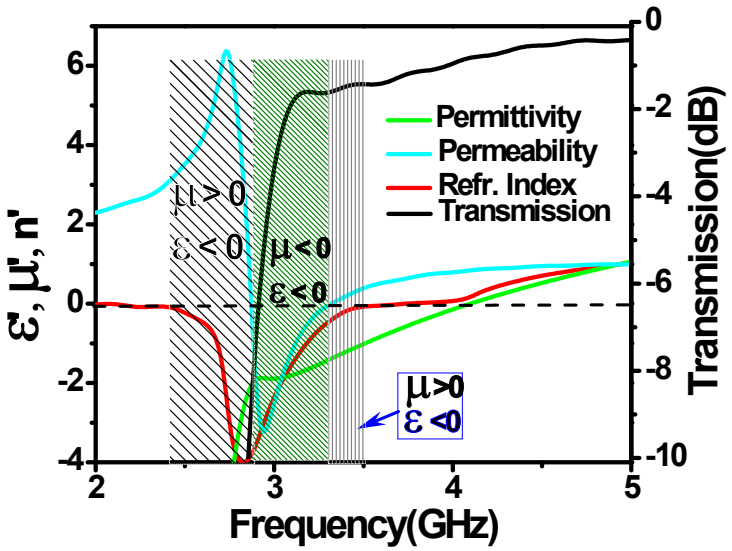

Figure 2.12 Graph showing refractive index, permittivity results, permeability results, and transmission graph of CMM array.

In order to get double negativity, magnetic resonance frequency of the structure should be less than plasma frequency of the structure. This condition is satisfied for this structure as can be seen in inset of fig. 2.12 where plasma and magnetic resonance frequencies are 4.1 and 2.94 GHz respectively.

Although there is not double negativity, refractive index is still negative in the inset of fig. 2.12, in the shaded frequency bands at the right and left sides of green shaded area. Therefore, double negativity is not a unique condition to get existence of negative refractive index[12, 14].

2.2.5 Cutwire-Wire array

Cutwire-wire structure is combination of cutwire structure with wire structure[9, 10, 42], in turn it is combination of negative permeability with negative permittivity in one structure. True choice of dimensions and plane wave orientation can result in negative refractive index. Like other negative refractive structures, this structure also should be transparent to electromagnetic wave in double negative frequency band (see fig. 2.16).

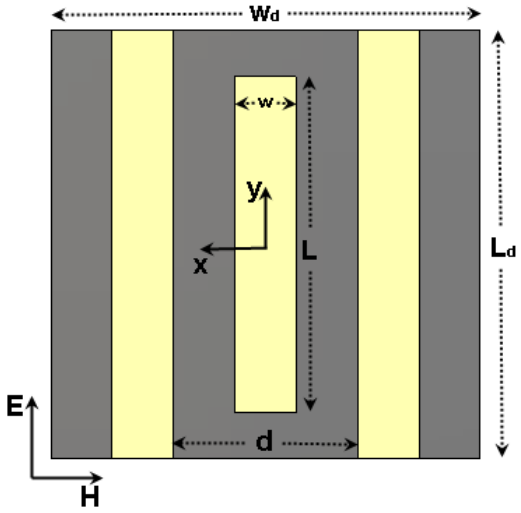

Figure 2.13 Schematic showing unit cell of cutwire-wire array.

A unit cell for cutwire wire array is shown in fig. 2.13. The dimensions of the structure used in the simulation are, w = 1 mm, L = 5.5 mm, d = 3 mm, L_d = 7 mm, w_d = 3.5 mm, t_m (thickness of metal) = 50 μm, t_d (thickness of dielectric) = 1 mm. Periodicities in x, y directions are 3.5 mm and 7 mm respectively. The structure is in x and y directions. Parameters of FR4 in between are $\varepsilon = 4.9$, $\mu = 1$ and $\delta = 0.025$. The orientation of electromagnetic wave sent is shown in fig. 2.13.

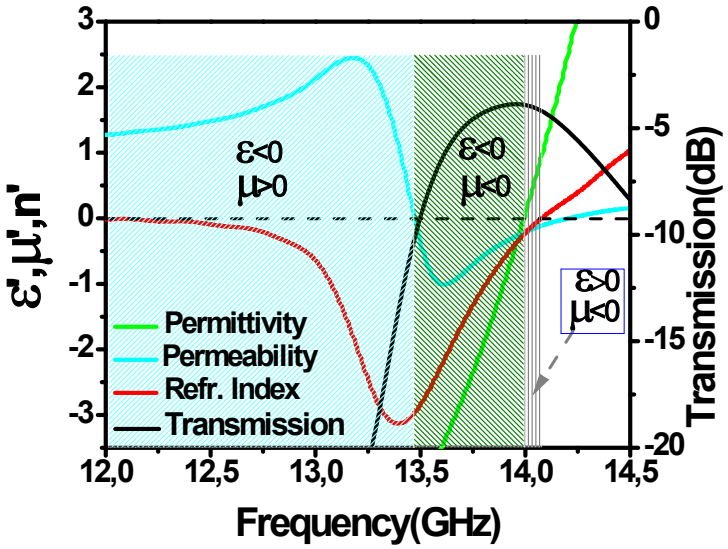

Figure 2.14 Graph showing refractive index, permittivity results, permeability results, and transmission graph of array.

Retrieval and transmission results of CMM array is shown in fig. 2.14. Shaded areas are in negative index region. As in the retrieval results of SRR-Wire CMM, there is negative refractive index band in which double negativity doesn't exist, in the inset of fig. 2.14. This result verifies non-uniqueness of double negativity to be necessary for left handedness.

Moreover, in the double negative region transmission result behaves as a passband, which verifies that in double negative region, a negative indexed material is transparent to electromagnetic waves.

2.2.6 Fishnet Structure

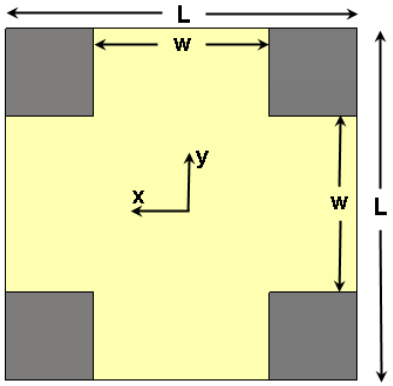

Figure 2.15 Schematic showing the one unit cell of fishnet structure.

Fishnet structure can possess negative refractive index when exited with normal to plane propagated wave, with true dimensions where should satisfy effective medium theory[13, 16]. This structure will be searched in detail, in next chapters.

CHAPTER 3

WHAT IS FISHNET STRUCTURE

3.1 Introduction

Fishnet structure is a planar metamaterial[13] structure. If the structure is left handed when propagation direction of incident wave is normal to plane of this structure, it is a planar metamaterial. Fishnet structure has some superior capabilities when compared with SRR-wire CMM. Firstly, fishnet is the only structure that is proven to have negative index at optical frequencies[12], and the magnetic response of SRR starts to saturate at optical frequencies[15], results in SRR-Wire array is not a suitable choice to be used as a LHM at optical frequencies. Secondly flexibility in manipulate of fishnet structure is easier than SRR-Wire CMM array at higher frequencies, because adding more layers to fishnet structure in propagation direction is easier than adding more layers to SRR structure in propagation direction.

3.1.1 *Variations of the fishnet structure*

The structure obtained by connecting of cutwire array with continuous wire array deposited on two faces of a dielectric board is called fishnet structure[10]. Some variations of symmetric and asymmetric fishnet structures possessing different geometric shapes were reported[16].

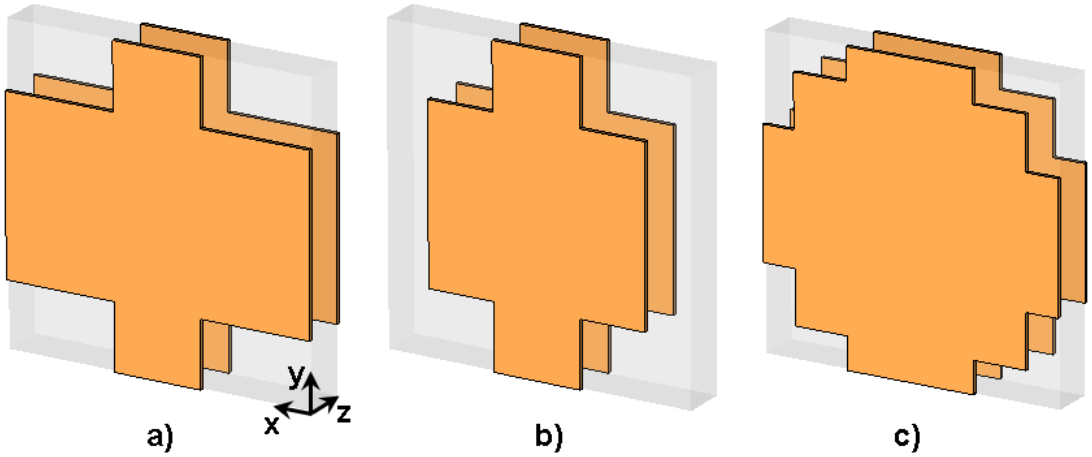

Figure 3.1 Schematics showing a) type-1, b) type-2, and c) type-3 of fishnet structure.

Unit cells of three types of fishnet structure are shown in fig. 3.1[16]. Type-2 and type-3 are modified versions of simple fishnet structure which is type-1. These modifications results in some benefits like 2-D fishnet engineering (type-2), and isotropic fishnet engineering (type-3).

3.1.2 *Equivalent circuit for fishnet structure in left-handed (LH) frequency band*

Fishnet structure can be modeled with an L-C circuit model[14, 16]. Inspecting electric and magnetic field distributions on metal part of fishnet structure in LH frequency band can be helpful to construct a circuit model. As a result of a plane wave sent to fishnet structure shown in fig. 3.1a, where electric field is parallel to y axis and magnetic field is parallel to negative side of x axis, E_z and, H_x distribution is shown in fig. 3.2.

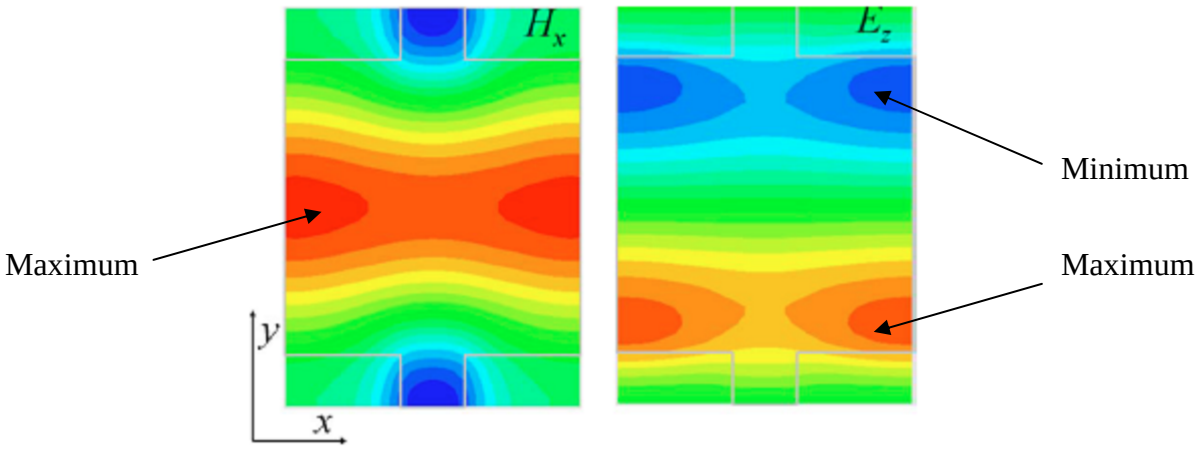

Figure 3.2 Schematics showing E_z and H_x distribution on one face of fishnet structure in fig. 3.1a where electric field is parallel to y axis and magnetic field is parallel to negative side of x axis. Areas denoting maximum and minimum field magnitudes are shown with arrows.

Magnetic field represents current (red and blue areas) and electric field in propagation direction (red and blue areas), which is E_z, represents electric charge. An analogy can be set between accumulation of electric charge and capacitor. Another analogy can be set between current and inductor[16]. Resulting equivalent fishnet circuit is shown in fig. 3.3.

Right and left sides of circuit in fig. 3.3a, represent equivalent circuits belonging to metal parts at different faces of fishnet structure respectively. Since there is symmetry in fishnet structure, *A* and *A'* nodes, *B* and *B'* nodes are equivalent nodes. As a result of symmetry of fishnet structure, circuit in fig. 3.3a can be transformed to another equivalent circuit shown in gif. 3.3b. One can assign numerical values to L and C in equivalent circuit in order to make detailed calculations.

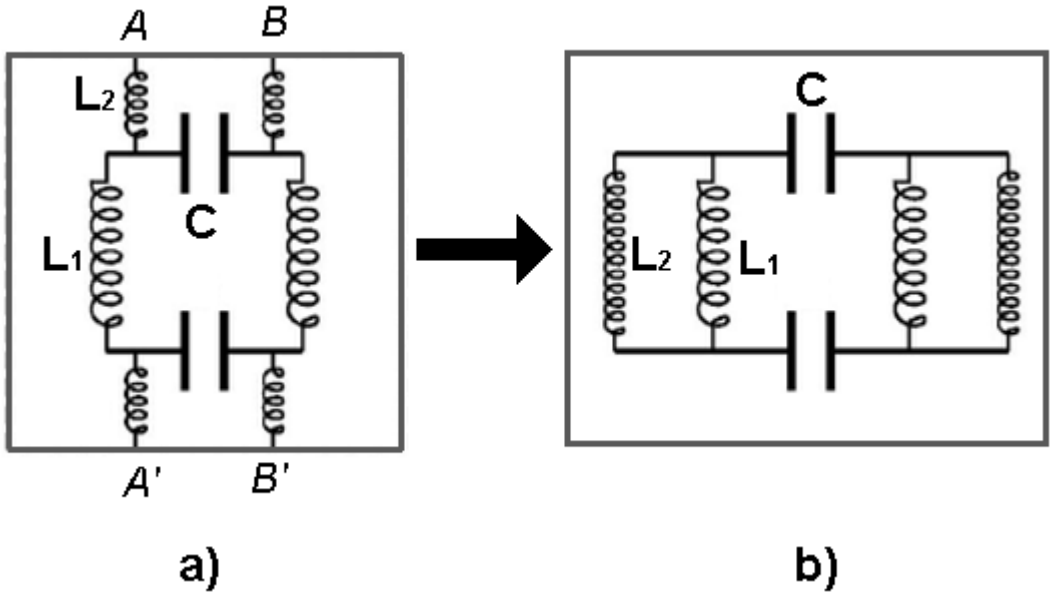

Figure 3.3 Schematics showing a) equivalent fishnet circuit, and b) corresponding equivalent fishnet circuit concerning with symmetry.

3.1.3 *Investigating left handedness of fishnet structure*

Transmission results of fishnet structure was obtained numerically or experimentally before[12, 17]. The LH region in transmission spectrum is denoted with a peak where there is a bandgap before this peak and there is a shoulder after this peak (see fig. 3.5). There are two types of condition to get left handedness at a frequency. One is existence of negative permittivity and negative permeability simultaneously (double negativity), and other is existence of only one of permittivity and permeability at a frequency. The condition in order to get refractive index of a medium negative is[12, 14]:

$$\varepsilon'\mu'' + \varepsilon''\mu' < 0 \qquad (3.1)$$

Where $(.)'$ and $(.)''$ denotes real and imaginary parts of any complex number, respectively. It is known that imaginary parts of permittivity and permeability should always be greater than zero. As a result of this and equation 3.1, at least one of real parts of permittivity and permeability should be negative in order to have negative index.

There are methods to understand whether a peak or a passband in a transmission spectrum of an effective medium is LH originated. One method is looking up retrieval results, and comparing it with transmission spectrum. If real part of refractive index at the frequency band corresponding to this peak or passband, this peak or passband denotes left handedness. Second method is to merge metal parts on two different faces of fishnet structure. This method kills magnetic resonance, in turn kills this peak denoting double negative left handedness, but still there is a possibility to get left handedness where real part of permittivity could be negative enough. Third method is comparing transmission phase spectra of different number of layered fishnet structures[17]. If one sees negative phase advance at a frequency region after this comparison, this structure is LH in this frequency region. Negative phase advance is also called backward wave propagation. Fourth method is investigating 2-D simulation results of a fishnet structure at a frequency[17]. If wave propagates along a direction in contrast with propagation direction of incoming wave through this structure at a frequency, this structure is LH at this frequency.

3.2 Left handedness in fishnet structure

3.2.1 *Double negativity of fishnet structure*

Three types of unit cells exist in order to construct a fishnet structure, as shown in fig. 3.4, where yellow parts are metal, and gray parts are dielectric.

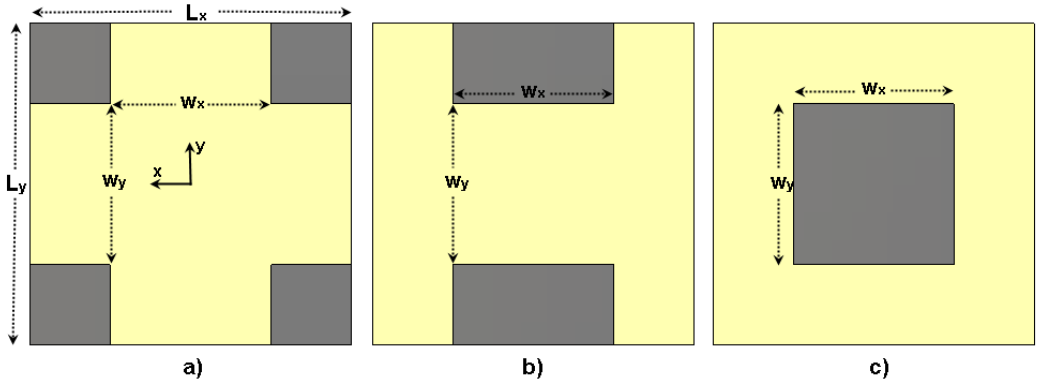

Figure 3.4 Schematics showing different unit cells to construct fishnet structure.

From the simulation results in CST Microwave Studio[44] the propagation direction is normal to fishnet plane where electric field is parallel to y axis. The parameters of the dielectric which is teflon are $\varepsilon = 2.16$, $\mu = 1$, and $\delta = 0.005$. Dimensions of the structure are $w_x = w_y = 7$ mm, $L_x = L_y = 14$ mm, and thicknesses of dielectric and metal are 1 and 0.02 mm respectively. The structure is periodic in x and y directions. Resulting transmission and retrieval spectra are shown in fig. 3.5.

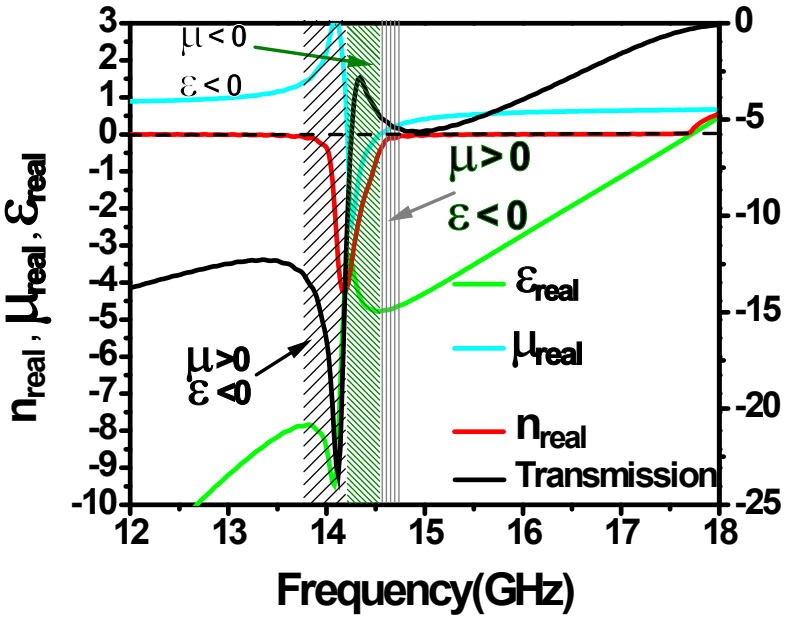

Figure 3.5 Graph showing refractive index, permittivity results, permeability results, and transmission graph of the one layer fishnet structure.

Inspecting fig. 3.5 gives us some data that, firstly, this structure is double negative in a narrow frequency band from 14.21 to 14.54 GHz, secondly the structure is left handed from 13.86 to 14.7 GHz.

3.2.2 *Experimental and retrieval verification of negative index of fishnet structure*

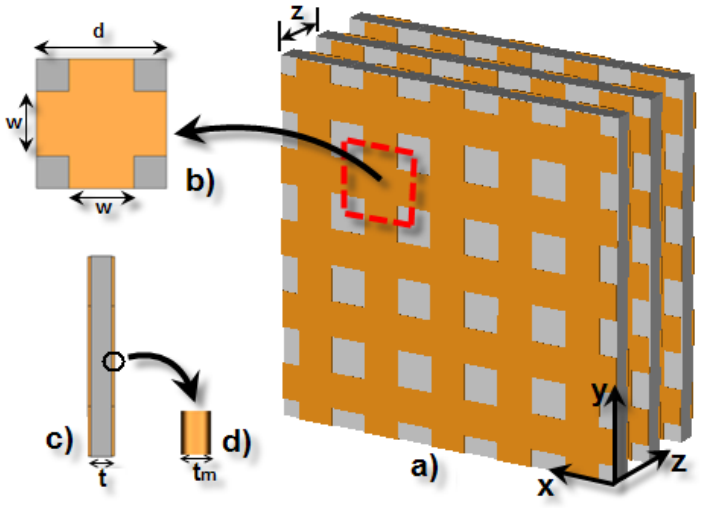

Figure 3.6 Schematics showing a) fishnet structure of which two sides are coated with copper, b) one unit cell of fishnet structure, c) side view of one unit cell, and d) side view of a copper part.

The fishnet structure is experimentally tested. The fig. 3.6 a, b, c, d shows fishnet structure, one unit cell of fishnet structure, side-view of one unit cell and side view of copper coated respectively. Dielectric used in structure is teflon which has constitutive parameters ε = 2.16, μ = 1, and δ = 0.005. The metal coated on dielectric is copper with a thickness (t_m) 30 μm. Fishnet unit cells are designed periodically with N_x = 10, N_y = 10 and N_z = 3 unit cells in x, y and z directions respectively. Periodicities of units in x, y, and z directions are a_x = 14 mm, a_y = 14mm, and a_z = 2 mm respectively. Dimensions of one unit cell which are symmetric due to x and y as shown in fig. 3.6b are, w = 7 mm, d = 14 mm. Thickness of dielectric (t) is 1 mm. Transmission measurements were done in free space with the experimental measurement setup consists of a HP 8510C network analyzer and a set of microwave horn antennas. The transmission results are calibrated with free space transmission in experiment. The wave excited is propagated in z direction and polarized in y direction.

A simulation for fishnet structure having same unit cell dimensions and constitutive parameters also was done in CST Microwave Studio[44]. In order to make the simulation easier, the unit cell was set periodic in x and y directions, with taking the same number of periodicity in z direction which is three. The propagation and polarization of wave excited with was remained same as the one in the experiment.

In addition to experiment and simulation, a retrieval code working in Matlab® used to obtain refractive index of this structure with using transmission results of simulation as input.

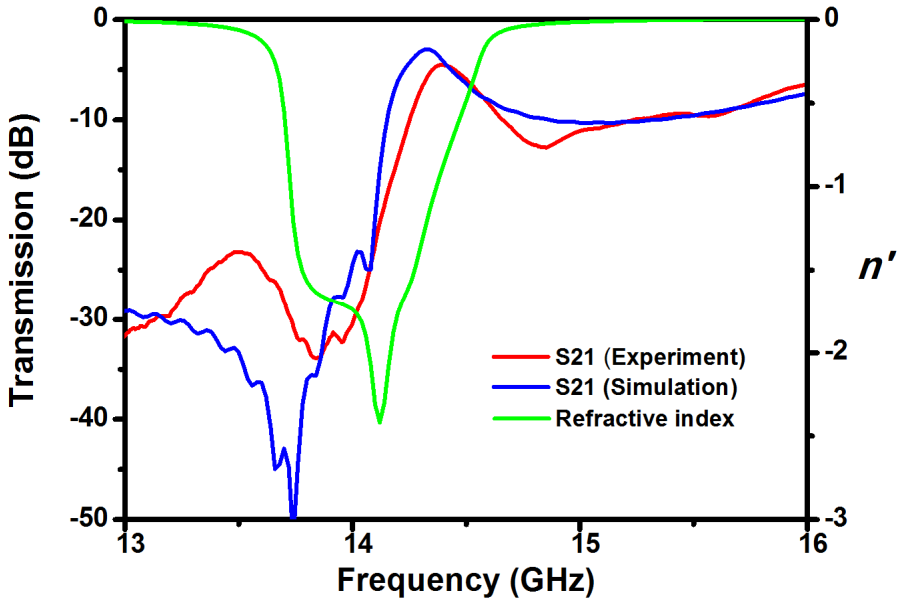

Figure 3.7 Graph showing the transmission results of experiment, transmission results of simulation, and real part of refractive index (n').

The results obtained after simulation, experiment and retrieval are shown in fig. 3.7. As can be seen clearly, experiment and transmission results are similar. Transmission peaks in experiment and simulation denotes that our structure has a negative refractive index that can be seen in fig. 3.7. Transmission peaks have magnitudes of -2.96 dB at 14.32 GHz in simulation, and -4.51 dB at 14.39 GHz in experiment. The structure has negative refractive index between 13.2 and 14.7 GHz with a minimum value of -2.42 at 14.12 GHz.

3.2.3 *Effect of change in polarization angle*

The fishnet structure investigated till here was symmetric structure. Another choice can be designation of an asymmetric structure when constructing fishnet structure.

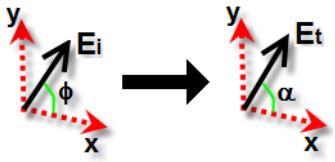

Figure 3.8 Schematic showing polarization of transmitted and incident wave travelling through an asymmetric fishnet structure.

What will happen if polarization of incoming normal to plane wave is an arbitrary angle? Some simulations were done in order to answer this question. The parameters and dimensions of fishnet structure are the same with the fishnet structure shown in fig. 3.4a, except w_y is widen from 7 mm to 9 mm, in the simulations done. This structure is asymmetric because $w_x \neq w_y$. In simulations done in order to analyze the relation between E_i and E_t is shown in figure 3.8 A normal to plane propagated planewave was sent to the structure where incident electric field magnitude is 1 V/m. Then, transmission results for x and y components of electric field at the output were obtained. As a result of inspection of transmission results, one can obtain magnitudes of x and y components of transmitted electric field for an incident electric field making an angle ϕ with x axis analytically with the knowledge of transmitted electric field when $\phi = 0°$ and transmitted electric field when $\phi = 90°$.

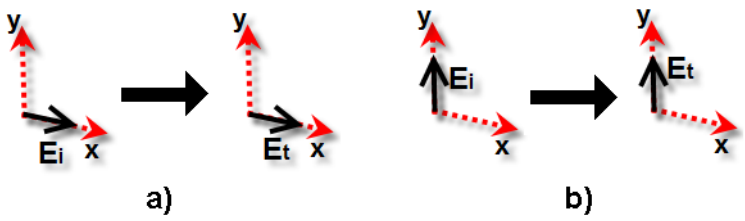

Figure 3.9 Schematic showing polarization of transmitted wave for x and y polarized electromagnetic wave.

In fig. 3.9, one can see that for an incident electric field parallel to x axis (ϕ = 0°), the transmitted electric field has only x component which has a magnitude $E_{0.}$ In addition, the transmitted electric field has only y component which has a magnitude E_{90} for an incident electric field parallel to y axis (ϕ = 90°).

As a result of intuition, the consequent formula giving transmitted wave for an incident electric field making an angle ϕ with x axis:

$$E_{t_x} = E_0 \cos\phi,\ E_{t_y} = E_{90} \sin\phi,\ E_t = \sqrt{{E_0}^2 \cos^2\phi + {E_{90}}^2 \sin^2\phi} \qquad (3.1)$$

The transmission results for ϕ = 0° (E_0), and ϕ = 90° (E_{90}) is shown in fig. 3.10.

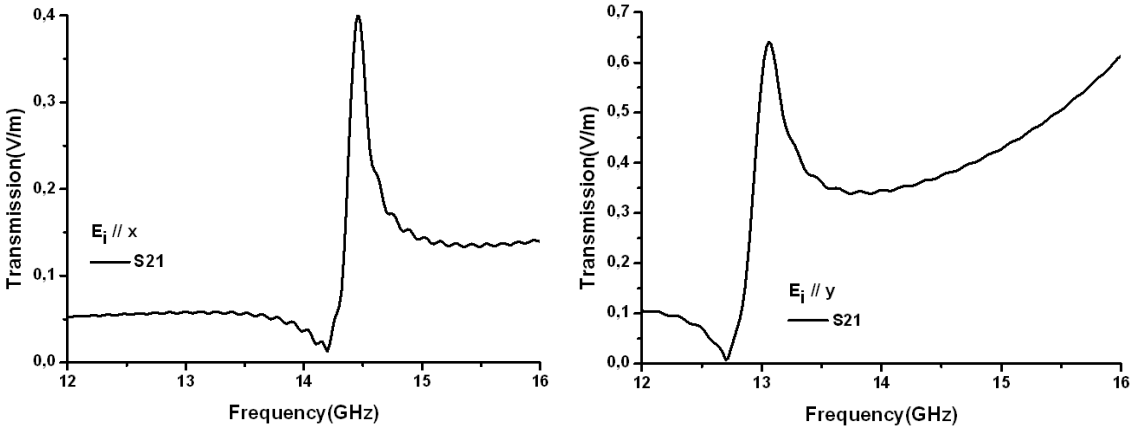

Figure 3.10 The transmission spectra for x polarized (the first one) and y polarized (the second one) electromagnetic waves.

As discussed above, one can calculate transmission result of any wave with propagation angle ϕ, by using data in fig. 3.8 and the eq. set 3.1. An example, when ϕ = 30°, transmission results calculated with eq. set 3.1 and simulation results are almost the same as can be seen in fig. 3.11.

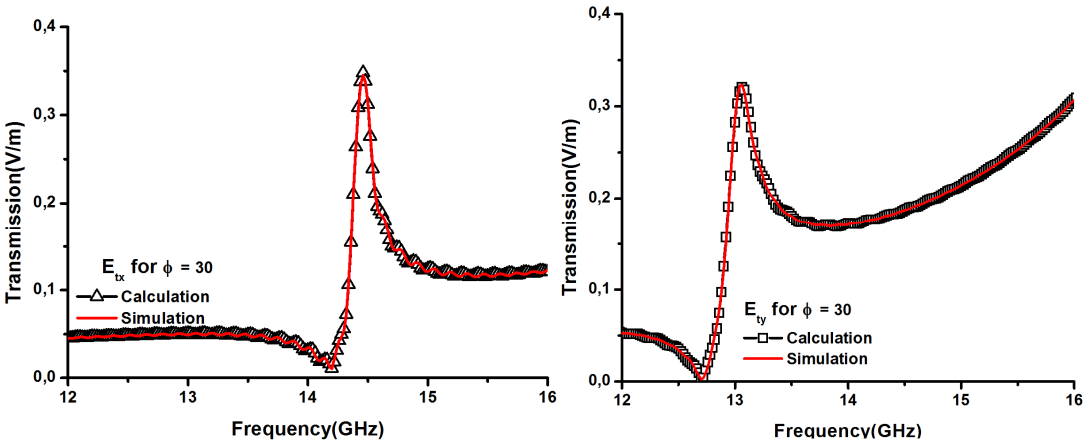

Figure 3.11 Graphs showing x (the first one) and y (the second one) components of calculated and simulated transmission spectra of incident electromagnetic wave with 30° propagation angle.

Therefore, fig. 3.11 proves equation set 3.1 unambiguously. One step ahead is equation 3.2 shown below.

$$\mathbf{E}_t = E_0 \cos\phi \hat{\mathbf{a}}_x + E_{90} \sin\phi \hat{\mathbf{a}}_y \qquad (3.2)$$

Which gives:

$$\tan\alpha = \frac{E_{90}}{E_0} \tan\phi \qquad (3.3)$$

Equation 3.3 shows an important result that α is not equal to ϕ without a case which is symmetric fishnet case. A unit cell of symmetric case and its dimensions was given in explanation of fig. 3.4. For this case, the equation of $E_0 = E_{90}$ is valid because of symmetry. Using equation 3.2 results in:

$$E_t = E_0 = E_{90} \qquad (3.4)$$

$$\alpha = \phi \qquad (3.5)$$

Notice that, there is no ϕ in equation 3.4. This promises that, magnitude of transmitted electric field does not depend on propagation angle of a normal to plane

incident wave in symmetric case. As a result of equation 3.5, polarization of a normal to plane incident plane wave doesn't change after the wave has transmitted through symmetric fishnet structure.

3.3 Parametric analysis of fishnet structure

Effects of any deviation from initial dimensions of fishnet structure on transmission result were searched with the aid of simulation. In these simulations, electric field is in y direction, and the incident wave is normal to plane propagated. In order to discuss results healthily, one should have some preliminary knowledge. A key knowledge is the continuous metal part parallel to electric field which is in y axis is responsible with plasma frequency[28, 29]. This continuous metal can be called as "wire". Another knowledge is, metal part parallel to magnetic field which is in x axis is responsible with magnetic resonance frequency. This metal part can be called as "slab". A structure having only slab part results in a resonance stopband in transmission spectrum[34]. Magnetic permeability is negative at this stopband which is a narrow band. A structure having only wire part results in a high frequency (HF) filter-like transmission spectrum which has a cut-off frequency called plasma frequency[38]. Plasma frequency is transition frequency between negative permittivity and positive permittivity. When wire and slab parts are combined in one structure results in a transmission peak at the intersection region of stopbands of only wire and only slab structures. This transmission peak denotes double negativity. The transmission peak of fishnet structure can be seen in fig. 3.5 (black line). In order to have an intersection of stopbands denoted with a peak in transmission spectrum, plasma frequency should be greater than resonance frequency. In addition, the shoulder touching zero dB at right side of transmission spectrum in fig. 3.5 denotes plasma frequency of fishnet structure.

Initial configuration of three layered fishnet structure is shown in fig. 3.12. w_x, w_y, L_x, L_y are dimensions of metals, then delX, delY and delZ are spatial periods of the fishnet. Electric and magnetic field directions are also shown in fig. 3.12.

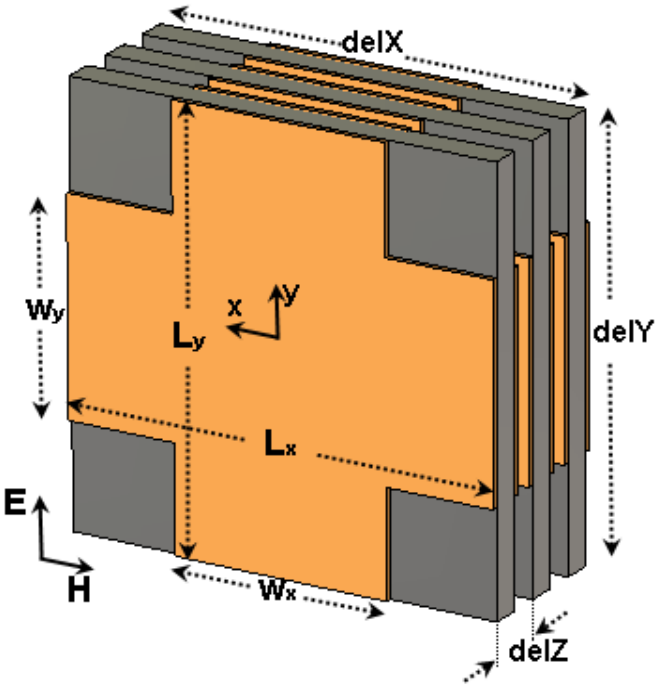

Figure 3.12 Schematic showing three layered fishnet structure and its parameters.

Initial dimensions of the structure are:

$w_x = w_y = 7$ mm

$L_x = L_y = 14$ mm

delX=delY=14 mm

delZ= 2 mm

Only one parameter is varied from initial dimension value of this parameter at every deviation step.

3.3.1 *w_x deviation*

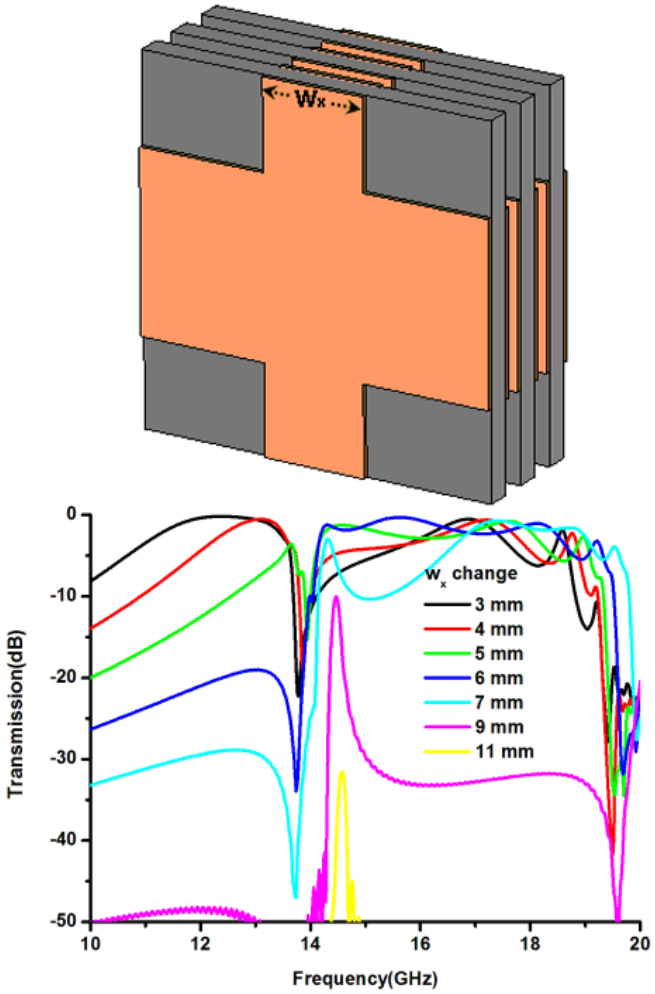

Figure 3.13 Schematic showing w_x deviated three layered fishnet structure and its transmission spectra.

When w_x is 3 mm, we don't see a transmission peak in fig. 3.13**.** The possible reason for this is plasma frequency is not bigger than resonance frequency yet. Increase in w_x increases positive difference between plasma frequency and resonance frequency, which results in a peak denoting double negativity, which is first seen when w_x = 6 mm in fig. 3.13. More increase in w_x starts to kill transmission, because the ratio of metal to overall structure is increasing with the increase of w_x, where metal is opaque to electromagnetic wave. In addition, this increase slightly increases frequency of transmission peak which is governed by resonance frequency, in turn, increase of w_x slightly effects resonance frequency of overall structure.

3.3.2 w_y *deviation*

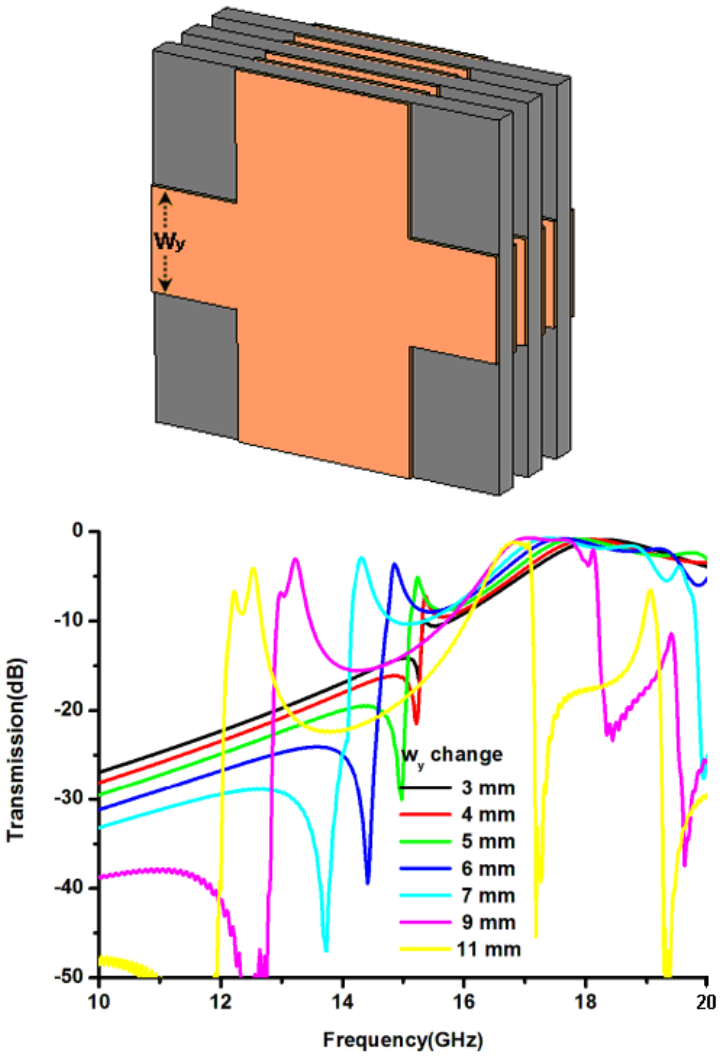

Figure 3.14 Schematic showing w_y deviated three layered fishnet structure and its transmission spectra.

As can be seen in fig. 3.14, increase of w_y decreases the frequency of transmission peak which means decrease in resonance frequency. Moreover, increase of w_y slightly shifts the shoulder at right side of resonance peak left, meaning decrease in plasma frequency slightly, in turn, w_y change also effects on plasma frequency even it is a slight effect.

3.3.3 L_x deviation

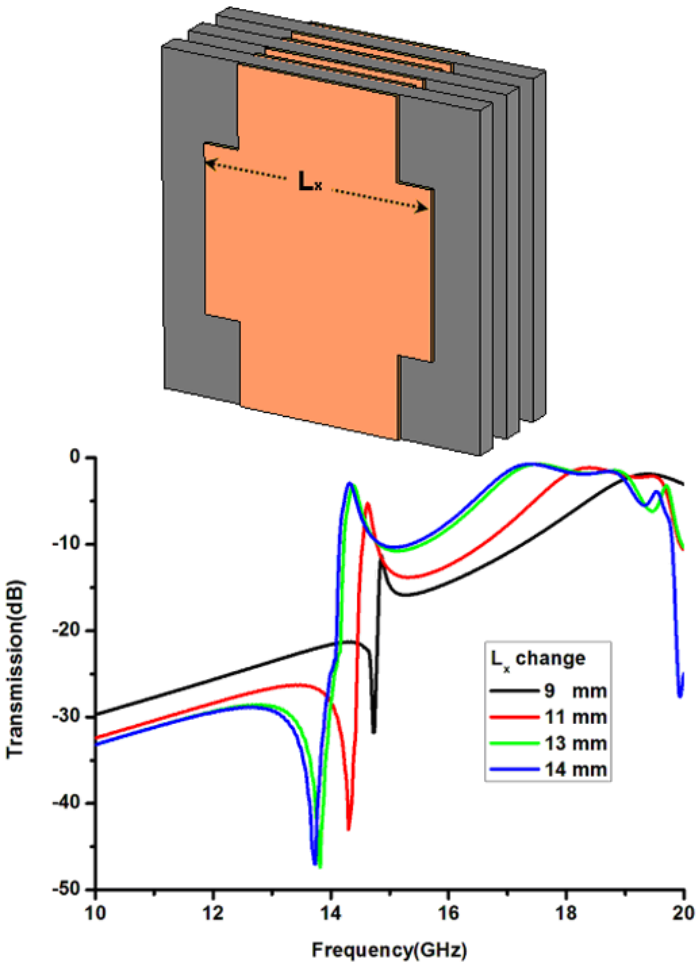

Figure 3.15 Schematic showing L_x deviated three layered fishnet structure and its transmission spectra.

Inspecting fig. 3.15 shows that, increase in L_x decreases plasma frequency which is denoted by shift of right shoulder to left, then, decreases frequency for transmission peak meaning that decrease in resonance frequency of this structure. And also, transmission peak increases with the increase of L_x.

3.3.4 L_y deviation

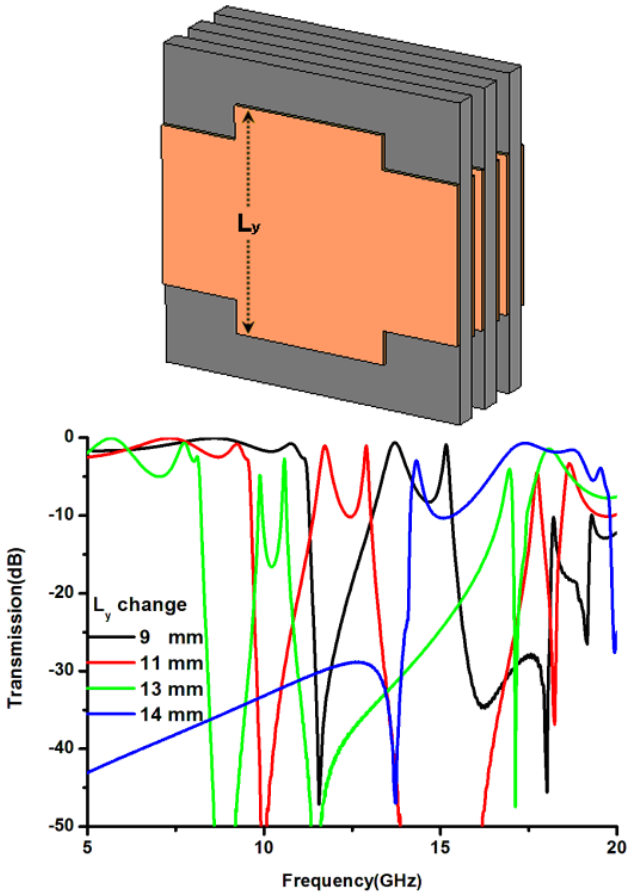

Figure 3.16 Schematic showing L_y deviated three layered fishnet structure and its transmission spectra.

There is no continuous wire on the structure in fig. 3.16 without the case when L_y = 14 mm. So, the structure is a modified cutwire structure in the cases without L_y = 14 mm case. Thus, the first bandgaps seen in fig. 3.16 without L_y = 14 mm case, is only result of magnetic resonance. These bandgaps shift upwards with the increasing of L_y, in turn, increase of L_y increases magnetic resonance frequency. An interesting point is, after increasing of resonance frequency with the increase of L_y, the bandgap transforms to a transmission peak near to 15 GHz when L_y reaches to 14 mm, because a continuous wire appears suddenly in addition to slab, in turn, double negativity comes to the screen with existence of wire denoting negative permittivity and slab denoting negative permeability simultaneously.

3.3.5 *delX* deviation:

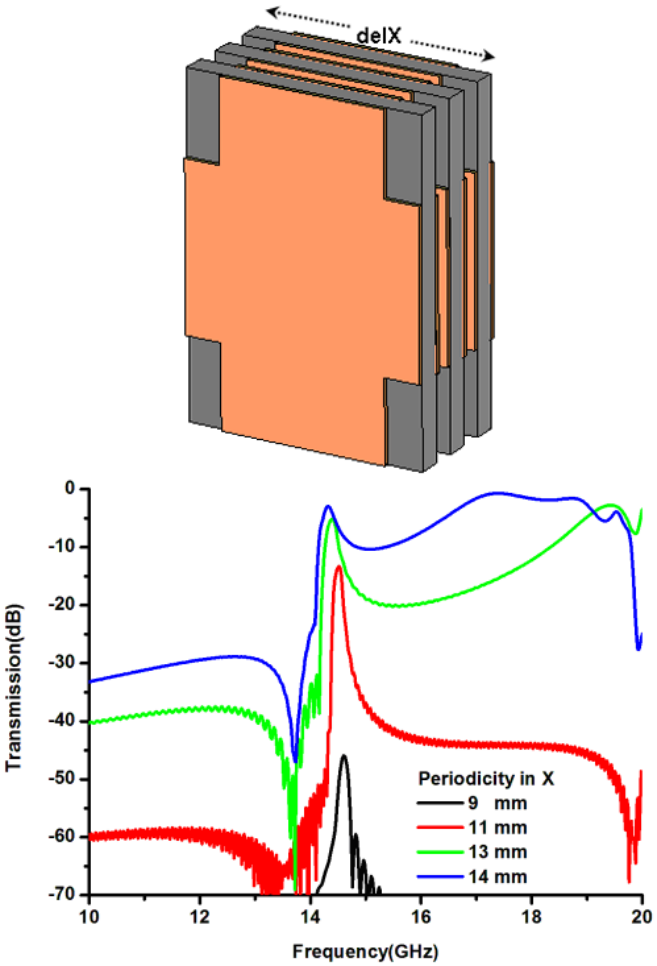

Figure 3.17 Schematic showing delX deviated three layered fishnet structure and its transmission spectra.

As can be seen in fig. 3.17, increase in periodicity delX decreases ratio of metal in structure, so raises transmission. A slightly decrease in frequency of transmission peak is seen with the increase of delX.

3.3.6 delY deviation:

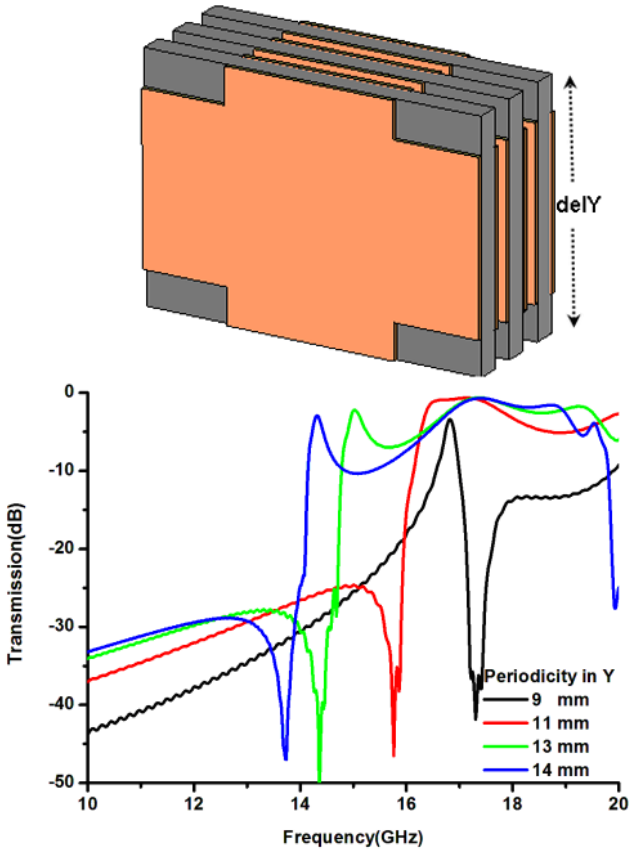

Figure 3.18 Schematic showing delY deviated three layered fishnet structure and its transmission spectra.

A double negativity response can not be seen when delY is 9 and 11 mm, then a transmission peak denoting double negativity exists when delY is 13 and 14 mm in fig. 3.18. The reason for this is, plasma frequency is not bigger than resonance frequency when delY is 9 and 11 mm. Increase in delY decreases resonance frequency which can be deducted from decrease in frequency of transmission peak. In addition, this increase results in increase of plasma frequency. Thus, the difference between plasma frequency and resonance frequency becomes positive, in turn, we have a transmission peak.

CHAPTER 4

NEGATIVE REFRACTION AND NEGATIVE PHASE ADVANCE IN FISHNET STRUCTURE

4.1 Inroduction

4.1.1 *Snell's law and wedge shaped prism*

A very embarrassing result of negative index is negative refraction. As known, refraction is the main law which governs how an electromagnetic wave is steered and manipulated through a matter. Capability of guidance of an electromagnetic wave with only positive refraction is incomplete. Investigation of negative refraction phenomena opened a new door to full control of steering or guiding an electromagnetic wave in a matter.

A right triangular wedge shaped medium can be used to analyze refractivity properties of the medium[31, 32]. The illustration showing path of an electromagnetic wave passing from a positive indexed wedge medium (PIM) to air is shown in fig. 4.1. The wave travelling in PIM bends towards clockwise direction (from red arrow to light blue one)[43].

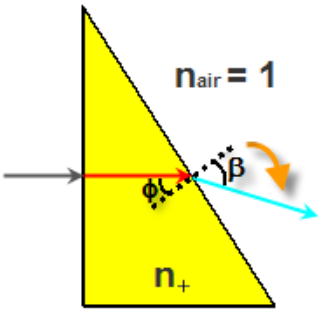

Figure 4.1 Schematic showing refraction ways of an electromagnetic wave for positive indexed wedge structure.

The expected ray that a wave should follow in a positive index medium is determined by Snell's law with taking index of air as 1.

$$n \sin \phi = \sin \beta \qquad (4.1)$$

The ray outgoing from negative indexed medium (NIM) should bend towards counterclockwise direction as illustrated in fig. 4.2. In order to prove this, one should change sign of refraction index in equation 4.1 where n is a positive number and α is refraction angle for a negative indexed medium:

$$-n \sin \phi = \sin \alpha \qquad (4.2)$$

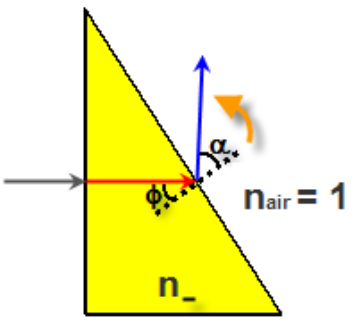

Figure 4.2 Schematic showing refraction ways of an electromagnetic wave for negative indexed wedge structure.

The result of combination of equations 4.1 and 4.2 is:

$$\sin\alpha = -\sin\beta \qquad (4.3)$$

Equation 4.3 shows that, refraction angle from a negative indexed medium is negative of refraction angle in positive indexed case, in turn proves that bending is towards counterclockwise direction in NIM case[30, 31].

4.2 Negative phase advance

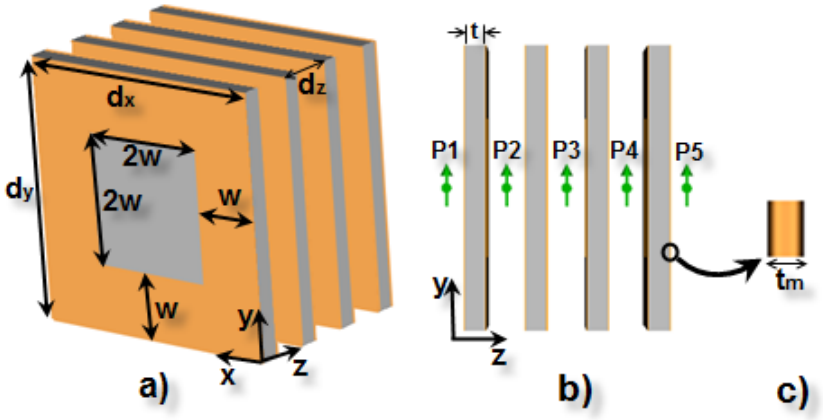

Figure 4.3 Schematics showing views from a) perspective, b) right side in simulation of fishnet structure, and c) side view of metal coated on two sides of dielectric.

One result of negative refractive index is negative phase advance which is an opposite behavior of naturally existing positive indexed materials[17]. In order to analyze this property in fishnet structure, a simulation was done in CST Microwave Studio[44], that schematics of simulation are shown in fig. 4.3. The structure is three layered and dimensions and periodicities were shown at the beginning of section 3.2. The wave sent to the structure is propagated in z direction and polarized in y direction. P1, P2, P3, P4, P5 shown in fig. 4.3.b are probes put in order to obtain transmission at different layers. Comparing arguments of transmissions at different layers is expected to show negative phase advance in fishnet structure.

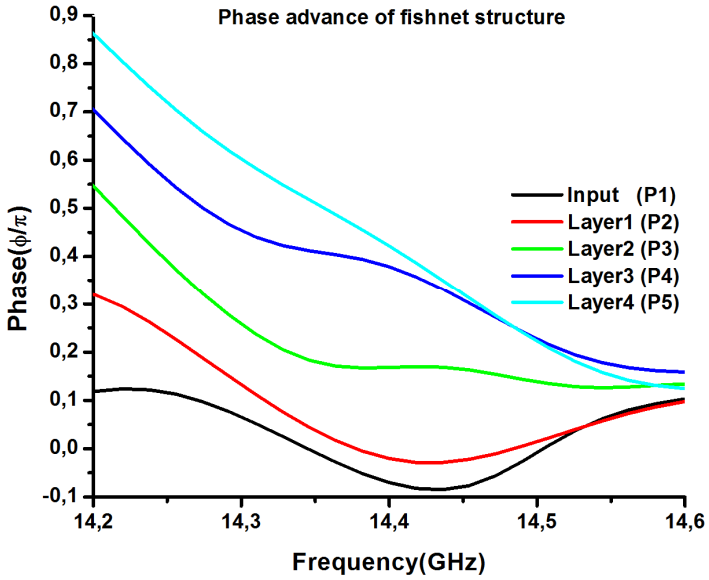

Figure 4.4 Graph for phase results at different layers of fishnet structure.

The resulting phase comparison graph is given in fig. 4.4. In order to be sure that it is negative phase advance, another simulation, which is different from previous one only in lack of metal. This means, only dielectric exists in the simulation. This simulation shows phase advance behavior of positive indexed medium.

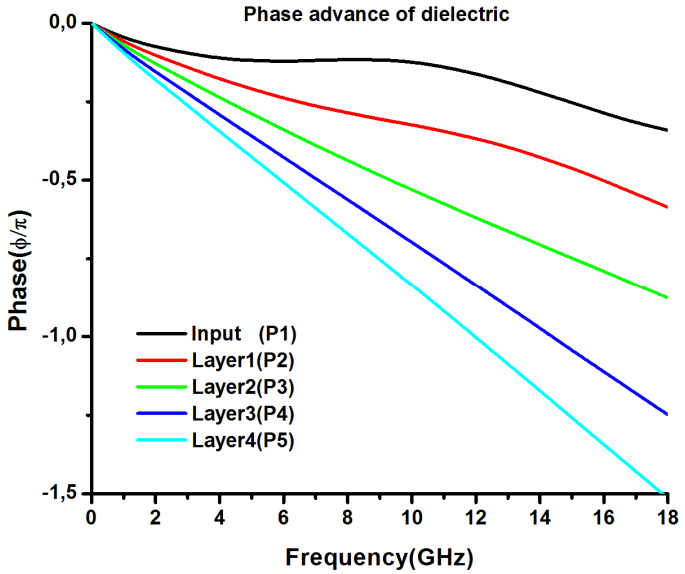

Figure 4.5 Graph for phase results at different layers of dielectric structure.

It can be clearly seen in inset of fig. 4.4 and 4.5, phase advance behavior of a wave propagating normal to plane in fishnet medium is opposite of its behavior when travelled through dielectric medium. This comparison gives that, a wave propagating normal to plane in fishnet structure has negative phase advance behavior. This property also called backward wave property.

4.3 Fishnet wedge structure

4.3.1 Refraction from fishnet wedge structure

Due to analyze refraction of fishnet structure further, a simulation of wedge structure made up of fishnet structure was done in CST Microwave Studio[44]. The wedge structure was built in the form that side view of the wedge is a triangle[30, 31]. The wedge structure is shown in fig. 4.6.

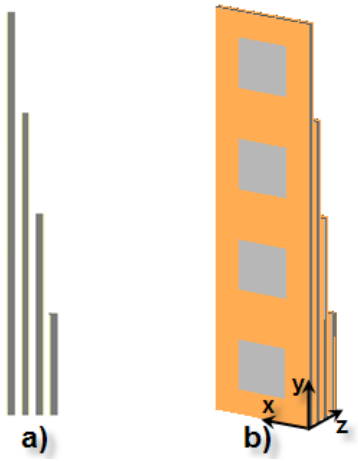

Figure 4.6 Schematics including a) side view, and b) perspective view of wedge structure constructed with fishnet unit cell.

In the wedge simulation, the wave was sent from the left side of fig. 4.6a, with a polarization in the x direction, and propagation in z direction. The structure shown in fig. 4.6 is periodic in x direction, and open in y and z directions in simulation. This structure is formed by arranging fishnet structures which are four layered, three layered, two layered and one layered in y direction. The constitutive parameters of metal, dielectric, periodicities and dimensions of a unit cell of fishnet structures were shown in section 3.2.

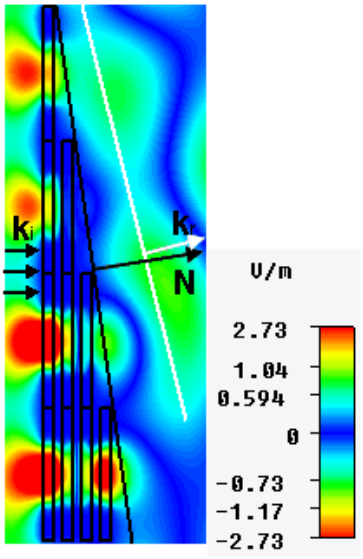

Figure 4.7 The 2-D snapshot for electric field of a plane wave travelling in a wedge.

In the wedge structure simulation, expected refraction ray was obtained at 14.33 GHz, as seen in fig. 4.7. The vector **N** in fig. 4.7 is normal vector for wedge structure, and vector **k** (subscript *i* is for incident wave, *r* is for refracted wave) is propagation vector. What we see in fig. 4.7 is, refracted wave vector stays at the counter clockwise side of normal vector as in fig. 4.2. Thus, comparing fig. 4.7 and fig. 4.2 gives that, this wedge structure has negative index at 14.33 GHz.

4.3.2 Phase advance in fishnet wedge structure

One of the results of negative refractive index is negative phase advance. Resulting 2-D graphs in fig. 4.8 for wave at 14.33 GHz (in negative index frequency region), and travelling through a fishnet wedge structure shows negative phase advance

clearly. As expected from a negative indexed structure, the wave travels through wedge structure from right side to left side, like in figure 4.8.

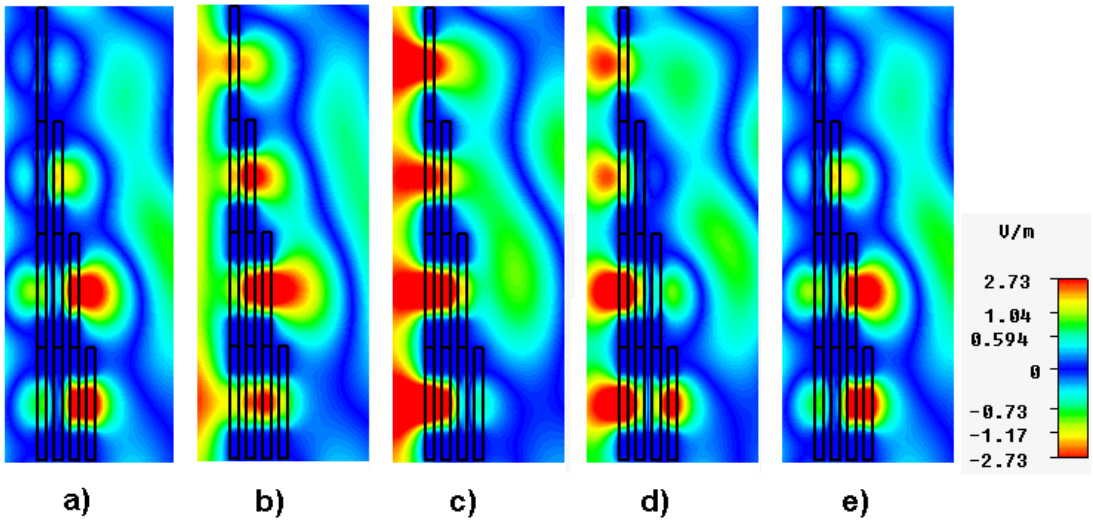

Figure 4.8 Sequential 2-D graphs showing phase advance through fishnet wedge structure at 14.33 GHz.

CHAPTER 5

DISORDER IN THE FISHNET STRUCTURES AND RESULTS

5.1 Introduction

In some cases an unexpected misalignment or disorder in an event may lead to fail any of expected advantageous results of this event, or may lead to some advantages results. In order to be saved from such unwanted results, or to be aware of advantageous results of misalignment, one should precalculate possible unexpected results could be, before it happened. Regarding this as a starting point motivates one to calculate or do experiments of possible disorders in order to see whether this disorder can destroy any expected benefit, or be used advantageously. This motivation led us to calculate numerically and do experiment of some disorders such as wire disorder, slab disorder and periodicity disorder along propagation direction that could happen in an application in which fishnet structure is used.

Some disorder calculations and experiments of some metamaterials were done before, and reported in literature[20, 21, 22, 23].

5.2 Disorder in fishnet structure

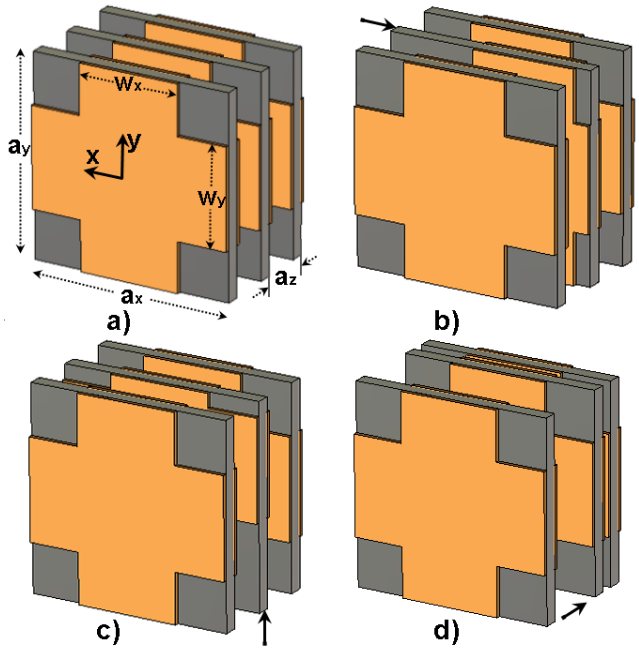

Figure 5.1 Schematics showing a) the ordered structure, b) the wire disordered structure (wire is the metal layer lying with electric field direction (y direction)), c) the slab disordered structure (Slab is the metal layer lying with electric field direction (y direction)), and d) non-periodic structure in z direction.

Transmission of fishnet structure (fig. 5.1a), then the effect of disorder on this transmission result was measured and calculated numerically (simulation). In order to achieve this, three type of disorders were given to this structure. First type of disorder is sliding the metal part which is called wire disorder (y-paralleled part), second type of disorder is sliding the metal part which is called slab disorder (x-paralleled part), then the third type of disorder is sliding whole middle layer in z direction called z disorder.

As discussed before, slab is responsible with effective magnetic permeability, and wire is responsible with effective electric permittivity. Thus, the expected result from misalignment of slab and wire disorders that it can affect effective magnetic permeability and permittivity respectively. In the case of disorder in z periodicity, coupling between succeeding layers can be effected.

5.2.1 *Ordered Fishnet Structure*

The unit cell for the fishnet structure measured is shown in fig. 5.1a. Dimensions of ordered structure and constitutive parameters of teflon board was shown in section 3.2.1. The periodicities of structure are $N_x = N_y = 10$ and $N_z = 3$, in experiment. The transmission measurements were done using a HP 8510C network analyzer and microwave horn antennas. The wave sent propagated towards direction **z**, and polarization was in **y** direction. Simulations were done by CST microwave studio[44]. The structures used in simulation were periodic in x and y directions.

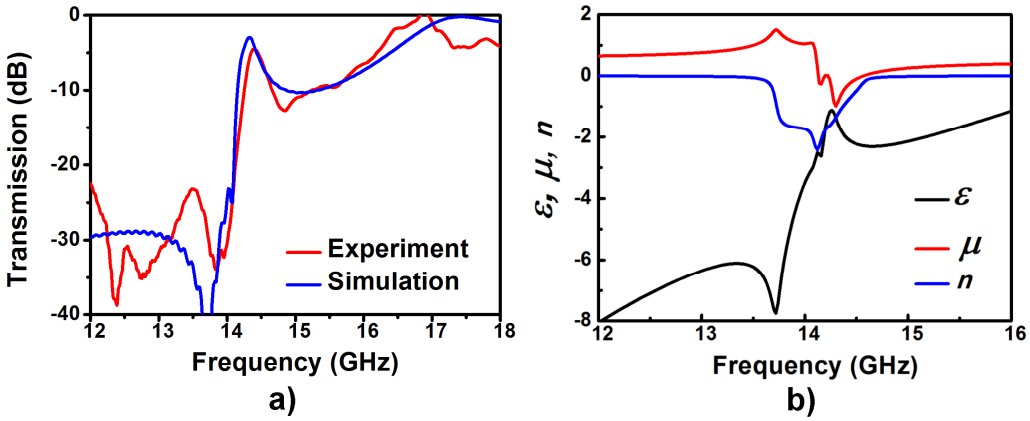

Figure 5.2 Graphs showing a) measurement and simulation results for ordered fishnet structure, and b) permittivity, permeability and refractive index for ordered fishnet structure.

The transmission results for simulation and experiment are shown in fig. 5.2a. The results are very close to each other as can be seen. The transmission peak of measurement for ordered structure is -4.47 dB at 14.38 GHz, and the transmission peak of measurement for ordered structure is -2.98 dB at 14.32 GHz. The resulting permittivity, permeability and refractive index spectrum of ordered structure are shown in fig. 5.2b. Minimum negative refraction is -2.4 at 14.12 GHz.

5.2.2 *Wire Disordered Fishnet Structure*

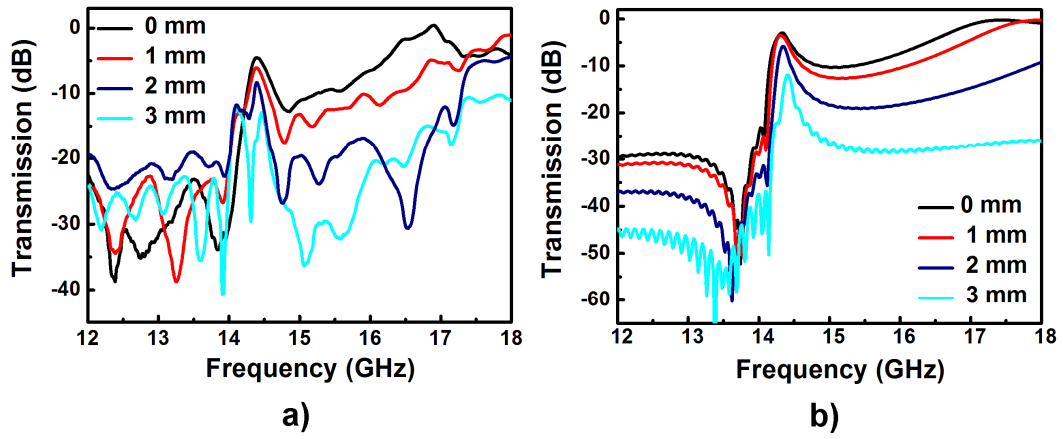

Figure 5.3 Graphs showing a) experimental results for 0mm (ordered), 1mm, 2mm, 3mm wire disordered structures, and b) simulation results for 0mm (ordered), 1mm, 2mm, 3mm wire disordered structures.

In order to achieve wire disorder, electric field paralleled metal part lying in y direction was slided in x direction. One can see wire disordered fishnet structure in fig. 5.1b. Experiment and simulation results of wire disordered fishnet structure are in fig. 5.3a and 5.3b respectively. Experiment and simulation results roughly agree with each other. Four types of order was chosen for wire disorder fishnet experiments and simulations which are 0mm disorder (ordered), 1mm disorder, 2mm disorder, 3mm disorder. The transmission peaks for experiment are -4.506 dB, -6.058 dB, -8.299 dB,-12.917 dB at 14.395 GHz, 14.385 GHz, 14.392 GHz, 14.467 GHz respectively. The transmission peaks for simulation are -2.963 dB, -3.516 dB, -5.816 dB, -11.917 dB at 14.32 GHz, 14.30 GHz, 14.34 GHz, and 14.40 GHz respectively. It can be inspected from transmission results that increase of wire disorder, results in decrease of transmission gradually. Another effect of wire disorder on transmission result is to increase peak frequency in small amounts. Increase in peak frequency denotes a positive shift in negative refractive index region.

5.2.3 *Slab Disordered Fishnet Structure*

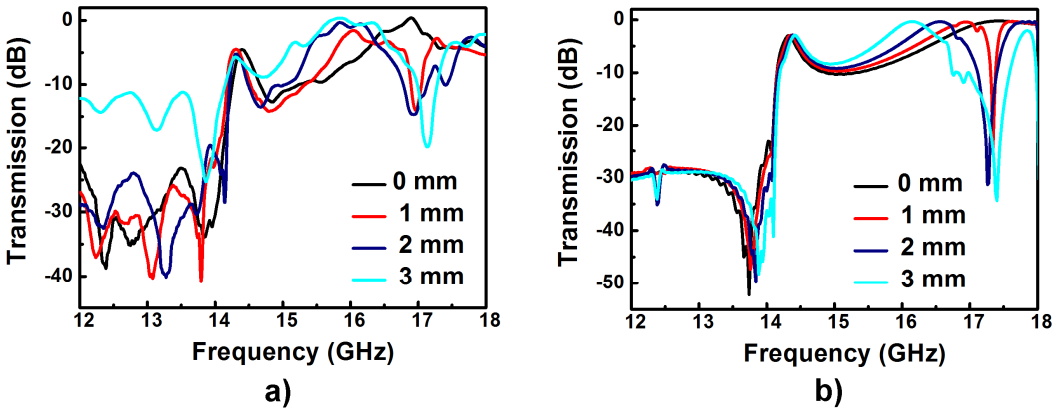

Figure 5.4 Graphs showing a) experimental results for 0mm(ordered), 1mm, 2mm, 3mm slab disordered structures, and b) Simulation results for 0mm(ordered), 1mm, 2mm, 3mm slab disordered structures.

Slab disorder in fishnet structure is shown in fig. 5.1c. One can see experiment and simulation results of slab disordered fishnet structure in fig. 5.4a and 4b respectively. Four types of order was chosen in experiment and simulations for slab disordered fishnet structure, as in wire disordered fishnet structure. The transmission peaks for experiment are -4.507 dB, -4.475 dB, -5.233 dB, -5.679 dB at 14.39 GHz, 14.31 GHz, 14.31 GHz, 14.30 GHz respectively. The transmission peaks for simulation are -2.963 dB, -2.932 dB, -2.870 dB, -2.887 dB at 14.32 GHz, 14.36 GHz, 14.38 GHz, 14.42 GHz respectively. It can be seen from transmission results for slab disordered fishnet structure, change in slab disorder doesn't change frequency of transmission peak. Moreover, disorder results in a new bandgap which has a center at 17.35 GHz approximately, and increase in disorder increases bandwidth of this bandgap. This bandgap could be originated from a magnetic or an electric resonance. If it is caused by a magnetic resonance, the reason of existence of a bandgap instead of a peak is lack of double negativity in this bandgap, because we expect a peak in a double negative region.

5.2.4 *Z Disordered Fishnet Structure*

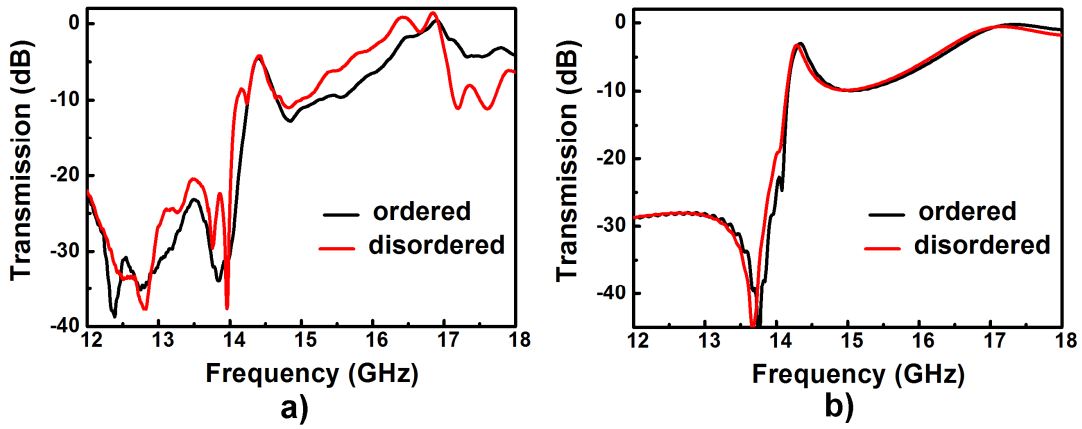

Figure 5.5 Graphs showing a) experimental results comparing ordered and z disordered (non-periodic in z direction) structures, and b) Simulation results comparing ordered and z disordered (non-periodic in z direction) structures.

Z disorder is non-periodicity in z direction as can be seen in fig. 5.1d. The experiment and simulation results of z disordered fishnet structure are in fig. 5.5a, 5b respectively. The experiment and simulation results are roughly meet each other. Inset of fig. 5.5a, and 5b shows that non-periodicity in z direction almost does not role in any change in transmission spectra for this structure. Transmission peaks for experiment are -4.507 dB, and -4.191 dB at 14.395 GHz, and 14.415 GHz respectively. The transmission peaks for simulation are -2.991 dB, and -3.265 dB at 14.34 GHz, and 14.28 GHz respectively.

Disorder in z periodicity almost doesn't change any part of transmission spectrum shown in fig. 5.5a and 5.5b.

5.2.5 *Retrieval Results*

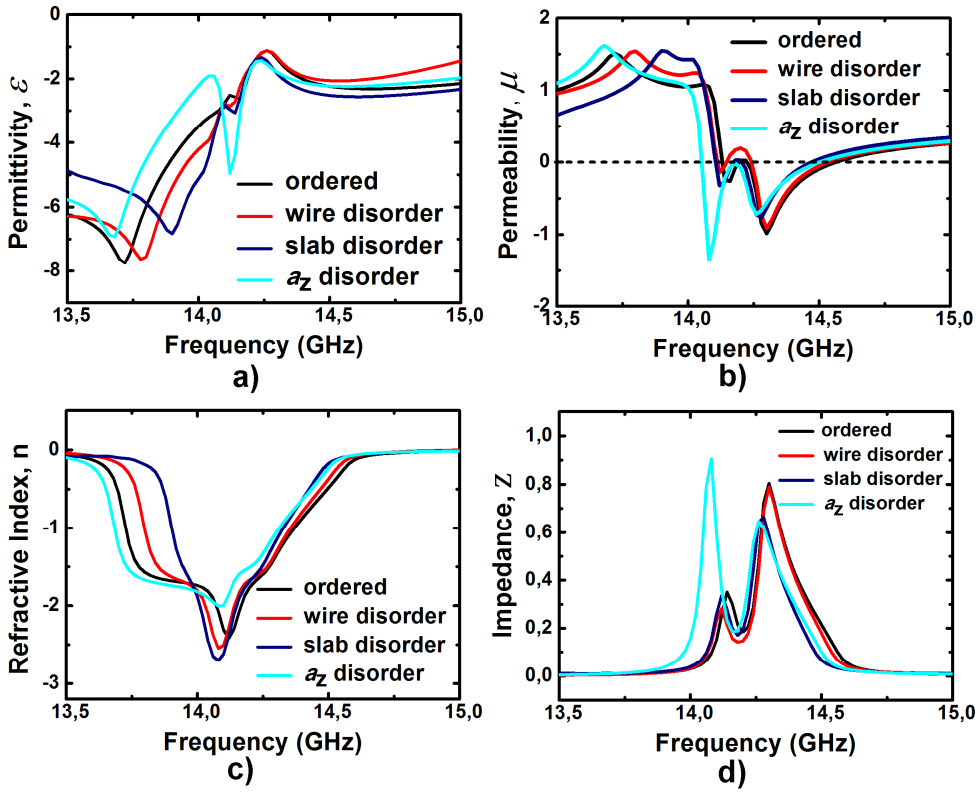

Figure 5.6 Comparison graphs of permittivity, permeability, refractive index, and impedance for all structures (ordered, wire disordered, slab disordered, z disordered structures).

The results seen in fig. 5.6 is for ordered structure, 1mm slided wire disordered fishnet structure, 1mm slided slab disordered fishnet structure, and z disordered fishnet structure. The inset of fig. 5.6 shows that, 1 mm disorders investigated here don't make a dramatic change in refractive index, so in left handedness, permittivity results, permeability results and impedance results of fishnet structure. However, in a sensitive application, one should behave cautiously in doing zero misalignment in order to avoid unwanted results.

CHAPTER 6

CONCLUSION

In this thesis, left handedness of fishnet structure analyzed with the aid of simulations, retrieval results and some experiments. This chapter is the conclusion chapter which summarizes thesis and discusses some results.

As a preparation, some matematerials and their negative properties, like permittivity, permeability and refractive index, reported in literature was discussed and supported with simulations and retrieval calculation results, in chapter-2.

Left handedness properties of fishnet structure were discussed in chapter-3. By using experimental, retrieval and simulation results; double negativity of fishnet structure was proved clearly. Then, relation between polarization of incident and transmitted wave was investigated, for fishnet structure. A formula for polarization dependence was discovered. It was shown that polarization angle doesn't change for a symmetric fishnet structure. Then, a parametric analysis of fishnet structure was done. In this analysis, results of variations in metal dimensions and variations in periodicities of different unit cell parameters were discussed.

Negative phase advance, and backward wave propagation through fishnet structure was proved with aid of simulation, in chapter-4. The comparison between phase advance results of four layered fishnet structure and four layered dielectric possessing positive refractive index was clearly showed that, phase advance through a fishnet structure is negative of phase advance occurring in natural materials. After that, 2-D result of transmission through a triangular wedge structure made by fishnet structure was discussed. This result clearly showed negative refraction through

wedge structure. Then, the negative phase advance through wedge structure was shown obviously with the aid of 2-D transmission snapshots.

Some possible disorders were shown and discussed in chapter-5. According to this discussion, wire disorder, which is shift of metal parallel to electric field, decreases transmission and, slightly increases magnetic resonance frequency. In addition, slab disorder, which is shift of metal parallel to magnetic field, almost doesn't change magnetic resonance frequency; however it creates a new bandgap widening with the increase of disorder. This new bandgap may be caused by a new magnetic or electric resonance.

REFERENCES

1) D. R. Smith, J. B. Pendry, M. C. K. Wiltshire, *Metamaterials and negative refractive index*, Science **305**, 788, 2004

2) Christophe Caloz, Tatsuo Itoh, *Metamaterials for high-frequency electronics*, Proceedings of IEEE **93**, 10, 2005

3) N. Seddon, T. Bearpark, *Observation of the inverse Doppler effect*, Science **302**, 1537, 2003

4) Costas M Soukoulis, Jiangfeng Zhou, Thomas Koschny, Maria Kafesaki, Eleftherios N Economou, *The science of negative index materials*, J. Phys. Condens. Matter **20**, 304217, 2008

5) V. A. Podolskiy, A. K. Sarychev, and V. M. Shalaev, *Plasmon modes and negative refraction in metal nanowire composites*, Optics Express **11**, 735, 2003

6) T. Koschny, M. Kafesaki, E. N. Economou, C.M. Soukoulis, *Effective medium theory of left-handed materials*, Phys. Rev. Lett. **93**, 107402 (2004)

7) J. B. Pendry, A. J. Holden, D. J. Robbins, and W. J. Stewart, *Low frequency Plasmons in thin-wire structures*, J. Phys. Condens. Matter **10**, 4785, 1998

8) V. D. Lam, J. B. Kim, S. J. Lee, Y. P. Lee, and J. Y. Rhee, *Dependence of the magnetic-resonance frequency on the cut-wire width of cut-wire pair medium*, Optics Express **15**, 16651 (2007)

9) Jiangfeng Zhou, Lei Zhang, Gary Tuttle, Thomas Koschny, and Costas M. Soukoulis, *Negative index materials using simple short wire pairs*, Phys. Rev. B **73**, 041101 (2006)

10) V. D. Lam, J. B. Kim, S. J. Lee, and Y. P. Lee, *Left-handed behavior of combined and fishnet structures*, Journal of Applied Physics **103**, 033107, 2008

11) Xudong Chen, Tomasz M. Grzegorczyk, Bae-Ian Wu, Joe Pacheco, Jr., and Jin Au Kong, *Robust method to retrieve the constitutive effective parameters of metamaterials*, Physical Review E **70**, 016608, 2004

12) Jiangfeng Zhou, Thomas Koschny, Maria Kafesaki and Costas M. Soukoulis, *Size dependence and convergence of the retrieval parameters of metamaterials*, PNFA **6**, 96, 2008

13) Kamil Boratay Alici, and Ekmel Ozbay, *A planar metamaterial: Polarization independent fishnet structure*, PNFA **6**, 102, 2008

14) Changchun Yan, Yiping Cui, Qiong Wang, and Shichuang Zhuo, *Negative refractive indices of a confined discrete fishnet metamaterial at visible wavelengths*, J. Opt. Soc. Am. B **25**, 1815, 2008

15) J. Zhou, Th. Koschny, M. Kafesaki, E. N. Economou, J. B. Pendry, and C. M. Soukoulis, *Saturation of magnetic response of split-ring resonators at optical frequencies*, Phys. Rev. Lett. **95,** 223902, 2005

16) M. Kafesaki, I. Tsiapa, N. Katsarakis, Th. Koschny, C. M. Soukoulis, and E. N. Economou, *Left-handed metamaterials: The fishnet structure and its variations*, Phys. Rev. B **75**, 235114, 2007

17) Koray Aydin, Zhaofeng Li, Levent Sahin, and Ekmel Ozbay, *Negative phase advance in polarization independent, multi-layer negative-index metamaterials*, Optics Express **16**, 8835, 2008

18) J. B. Pendry, *Negative Refraction makes a perfect lens*, Phys. Rev. Lett. **85,** 3966, 2000

19) D. Schurig, J. J. Mock, B. J. Justice, S. A. Cummer, J. B. Pendry, A. F. Starr, and D. R. Smith, *Metamaterial Electromagnetic Cloak at Microwave Frequencies*, Science **314**, 977, 2006

20) Alexander A. Zharov, Ilya V. Shadrivov, and Yuri S. Kivshar, *Suppression of left-handed properties in disordered metamaterials*, Journal of Applied Physics **97**, 113906, 2005

21) Thomas Hand, Soji Sajuyigbe, Shawn Mendonca, Steve Cummer, and David R. Smith, *Characterizing the effects of disorder in metamaterial structures*, Applied Physics Letters **91**, 162907, 2007

22) Maxim V. Gorkunov, Sergey A. Gredeskul, Ilya V. Shadrivov, and Yuri S. Kivshar, *Effect of microscopic disorder on magnetic properties of metamaterials*, Phys. Rev. E **73**, 056605, 2006

23) Koray Aydin, Kaan Guven, Nikos Katsarakis, Costas Soukoulis, and Ekmel Ozbay, *Effect of disorder on magnetic resonance band gap of split-ring resonator structures*, Optics Express **12**, 5896, 2004

24) VG Veselago, *The electrodynamics of substances with simultaneously negative values of permittivity and permeability*, Sov. Phys. Usp. **10**, 504, 1968

25) J. B. Pendry, A. J. Holden, W. J. Stewart, and I. Youngs, *Extremely Low Frequency Plasmons in Metallic Mesostructures*, Phys. Rev. Lett. **76**, 4773, 1996

26) J. B. Pendry, A. J. Holden, D. J. Robbins, and W. J. Stewart, *Magnetism from Conductors and Enhanced Nonlinear Phenomena*, IEEE Trans. Microwave Theory Tech. **47**, 2075, 1999

27) D. R. Smith, Willie J. Padilla, D. C. Vier, S. C. Nemat-Nasser, and S. Schultz, *Composite Medium with Simultaneously Negative Permeability and Permittivity*, Phys. Rev. Lett. **84**, 4184, 2000

28) Koray Aydin and Kaan Guven, Maria Kafesaki, Lei Zhang and Costas M. Soukoulis, Ekmel Ozbay, *Experimental observation of true left-handed transmission peaks in metamaterials*, Optics Letters **29**, 2623, 2004

29) Mehmet Bayindir, K. Aydin, E. Ozbay,P. Markos, C. M. Soukoulis, *Transmission properties of composite metamaterials in free space*, APL **81**, 120, 2002

30) Kaan Guven, Koray Aydin, Ekmel Ozbay, *Experimental analysis of true left-handed behaviour and transmission properties of composite metamaterials*, PNFA **3**, 75, 2005

31) Koray Aydin, Kaan Guven, Costas M. Soukoulis, Ekmel Ozbay, *Observation of negative refraction and negative phase velocity in left-handed metamaterials*, APL **86**, 124102, 2005

32) Z. G. Dong, S. N. Zhu, H. Liu, J. Zhu and W. Cao, *Numerical simulations of negative-index refraction in wedge-shaped metamaterials*, Physical Review E **72**, 016607, 2005

33) D. Schurig, J. J. Mock, B. J. Justice, S. A. Cummer, J. B. Pendry, A. F. Starr, D. R. Smith, *Metamaterial Electromagnetic Cloak at Microwave Frequencies*, Science **314**, 977, 2006

34) Vladimir M. Shalaev, Wenshan Cai, Uday K. Chettiar, Hsiao-Kuan Yuan, Andrey K. Sarychev, Vladimir P. Drachev, and Alexander V. Kildishev, *Negative index of refraction in optical metamaterials*, Optics Letters **30**, 3356, 2005

35) Nicholas Fang, Xiang Zhang, *Imaging properties of a metamaterial superlens*, APL **82**, 161, 2003

36) D. R. Smith, S. Schultz, P. Markos, C. M. Soukoulis, *Determination of effective permittivity and permeability of metamaterials from reflection and transmission coefficients*, Physical Review B **65**, 195104, 2002

37) Ekmel Ozbay, Zhaofeng Li, Koray Aydin, *Super-resolution imaging by one-dimensional, microwave left-handed metamaterials with an effective negative index*, J. Phys. Condens. Matter **20**, 304216, 2008

38) Peng L, Ran L, Chen H, Zhang H, Kong J A, Grzegorczyk T M, *Experimental Observation of Left-Handed Behavior in an Array of Standard Dielectric Resonators*, Phys. Rev. Lett. **98**, 157403, 2007

39) D. R. Smith, D. C. Vier, Th. Koschny, C. M. Soukoulis, *Electromagnetic parameter retrieval from inhomogeneous metamaterials*, Physical Review E **71**, 036617, 2005

40) Koray Aydin, Ekmel Ozbay, *Experimental and numerical analysis of the resonances of split ring resonators*, Phys. stat. sol. B **244**, 1197, 2007

41) J. Lu, T. Grzegorczyk, Y. Zhang, J. Pacheco Jr., B. Wu, J. Kong, M. Chen, Optics Express **11**, 723, 2003

42) T. F. Gundogdu, N. Katsarakis, M. Kafesaki, R. S. Penciu, G. Konstantinidis, A. Kostopoulos, E. N. Economou, and C. M. Soukoulis, *Negative index short-slab pair and continuous wires metamaterials in the far infrared regime*, Optics Express **16**, 9173, 2008

43) Andrew A. Houck, Jeffrey B. Brock, Isaac L. Chuang, *Experimental Observations of a Left-Handed Material That Obeys Snell's Law,* Physical Review Letters **90**, 137401, 2003

44) User Manual, Version 5.0, CST GmbH, Darmstadt, Germany, http://www.cst.de, Last visit on 09 March 09